Parametric tools for the analysis of micro-architectured thin structures

Cristina Capdevila Choy

School of Engineering

Thesis submitted for examination for the degree of Master of Science in Technology.

Espoo July 29, 2019

Thesis supervisor:

Asst. Prof. Jarkko Niiranen

Thesis advisor:

Dc.Sc. Viacheslav Balobanov

Aalto University
School of Engineering

Aalto University
School of Engineering

Aalto University, P.O. BOX 11000, 00076
AALTO
www.aalto.fi

Abstract of master's thesis

Author Cristina Capdevila Choy

Title of thesis Parametric tools for the analysis of micro-architectured thin structures

Master programme Building Technology **Code** ENG27

Thesis supervisor Assistant Professor Jarkko Niiranen

Thesis advisor(s) Doctor of Science Viacheslav Balobanov

Date 29.07.2019 **Number of pages** 55 + 3 **Language** English

Abstract

The present work is devoted to a tool for generating lattice structure geometries. A review on lattice structures is performed passing through their definition, history and actual fields of applicability. An overview of software that is currently available for lattice geometries generation and their finite elements analysis is also accomplished, including the software pros and cons in the context of the research purposes of the present work.

Based on the review, a scripted tool is developed and implemented boosting user customization and future FEA integration as a software prototype. An explanation of the generalized idea, structure and organization is given. The validation of the tool has been executed through a banch of examples.

The applicational potential of the tool in modelling and analysis of different lattice structures made of the different RVEs is demonstrated including the simulation of possible imperfections arising due to manufacturing defects. In addition, it is shown how the tool can help in homogenization of the artificial micro-architectural lattice materials accomplished with the aid of the gradient elasticity theory.

Keywords Cellular Structures, Finite Element Analysis, Lattice structures, Lightweight structures, Micro-architectured material and Strain Gradient Elasticity.

Preface

This work has been accomplished at The Department of Civil Engineering, Aalto University during my exchange period Polytechnic University of Catalonia grant me. First of all I would like to express my gratitude to both institutions to provide me the knowledge now I have. Moreover, I would like to thank my Supervisor and my Advisor Assistant Professor Jarkko Niiranen and Doctor in Science Viacheslav Balobanov, respectively, to guide me and help me during this thesis work. Moreover, I would like to mention the contribution of Professor Antonio Rodriguez Ferran for his advice and recommendations in times of uncertainty of the process. I want also to thank Teacher Djebar Baroudi that without any intention has accompanied me in these long days and weekends of work in the Departmant. Concluding, I would like to expose my appreciation for the support my friends and also my family, from far away, unconditionally gave me. Finally, I do not forget my mum who, from a star, is always sending me energy to accomplish my goals.

Otaniemi, July 29, 2019

Contents

Abbreviations

AM	Additive Manufacturing
CAD	Computer Aided Design
CAE	Computer Aided Engineering
CAM	Computer Aided Manufacturing
FEA	Finite Element Analysis
FEM	Finite Element Method
LNG	Lattice Net Generator
MEMS	Microelectromechanical Systems
NEMS	Nanoelectromechanical Systems
RVE	Representative Volume Elements

1 Introduction

1.1 Cellular materials

Cellular materials were started to be used many centuries ago for manifold applications inspired by their presence in natural materials such as wood, coral, honeycombs and many others [23]. The material is considered to be a structure of beams or (curved) surfaces that organize forming edges and faces and setting up a repeating cell [23]. More recently, during the industrial revolution, these materials have been given multiple specific uses such due to their impressive properties such as weight reduction, heat transfer, thermal insulation and energy absorption [12, 21, 30, 35]. In the beginning, the fabrication methods required special techniques that involved solid state processing and vapor deposition. Only randomly organized structures could be created and pore size and density were the only characteristics that could be controlled [9, 39]. Additive manufacturing (AM) arose in the late 90's bringing the layer-by-layer manufacturing archetype. This technique provides control over the cell of the structure i.e. internal and external material architecture. Typically, these structured materials are called lattice structures which, without losing the possibility to be randomly pattered, they are mostly considered to have non-stochastic topology instead.

Currently, lattice structures design is on focus in many fields due to a great extent of novel capabilities of 3D printing. These technologies allow to create very complex geometries that were impossible in the past. As the world becomes more competitive, multiple industries are looking to create high quality and economic materials and lattice structures bring this possibility [51]. For instance, this structures can provide a high stiffness-weight ratio or a high surface-volume ratio while reducing the material wastage [17].

Lattice materials are used to replace solid volumes, as they can fulfill the design requirements with significantly less weight. As mentioned, in structural design they provide a high stiffness-weight ratio being actually on the eye of many engineering disciplines like the aerospace or the bio-engineering. Other attractive properties are the energy absorption under compressive and dynamic loading [12, 21, 29, 32, 55], the high heat conductivity [27, 56] and the great noise and vibration transmission [3, 31, 52].

New models tie lattice structures with topology optimization. This paradigm is used to provide an optimized material distribution for a structure. They aim to satisfy a given design load, being mechanical [11, 19, 34, 61], thermal [56] or also, vibrational [52]. Recently, ground truss structure approaches have been studied for topology optimization [24, 40, 58]. They usually employ heuristic methods, starting with a design space and a predefined unit cell type, then defining single or multiple design variables that are optimized for the desired stress states.

Nowadays, there is the possibility to design and manufacture unfettered complex lattice structures. It requires appropriate theories to describe their performance. Hence, one can go through the exploration and harnessing of their properties and qualities. Nevertheless, they are sophisticated structures that are showing outstanding properties, and their explaining challenge the scientific and engineering community. Usually, models need to be simplified so as to be feasible from a computational point of view.

1.2 Micro-architectured thin structures

Micro-architectured thin structures have been deeply studied. Micro-architectured materials can be considered as hybrid materials, combinations of two or more materials, or of materials and space, integrated in such a way that unique material properties can be obtained with them [74]. Examples of these materials are sandwich structures, foams, lattice structures, segmented structures, zero expansion materials, and more a classification proposed on [4] is shown in figure 1. The concept of architectured material comes from the desire to "put material only where it is needed" [45]. The following diagram shows the behaviour of lattice compared to other materials, figure 2.

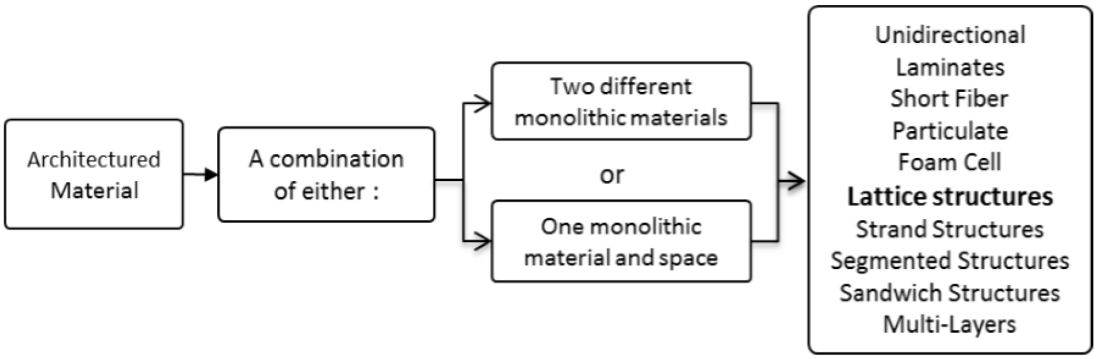

Figure 1: Architectured materials. Source: [4].

Note that lattices are considered configure materials when the wavelength of any loading is much longer than the lattice elements. On the other hand, the lattices are considered structures when the number of lattice elements inside and the length scale of the loading are not comparable to the lattice element [21**?**].

An important differentiation of lattice structures is in bending or stretch-dominated mechanical performance. Bending-dominated lattice structures show high stiffness and energy absorption, however lowering the overall strength [5]. Oppositely, stretch-dominated lattice structures are particularly strong and stiff. This behavior is reflected in the compressive stress-strain diagram shown in figure 2 and figure 4 which introduce bending and stretching dominated lattices in the Ashby diagram of Young modulus vs. density.

Maxwell Stability Criterion and the associated Maxwell Number, M, is used to evaluate weather a lattice is stretching or bending dominated. In case of 3D lattices it is calculated as follows: $M = m - 3 \cdot n + 6$ being m the number of bar elements and n the number of nodes of the lattice cell. For bending dominated lattices $M < 0$, otherwise they are considered stretch dominated structures or over-stiff. In case of 2D structures (planar), the equation is changed to $M = m - 2 \cdot n + 3$ [5, 38, 44, 48, 74]. Figure 5 shows some examples of stretch and bending dominated lattices.

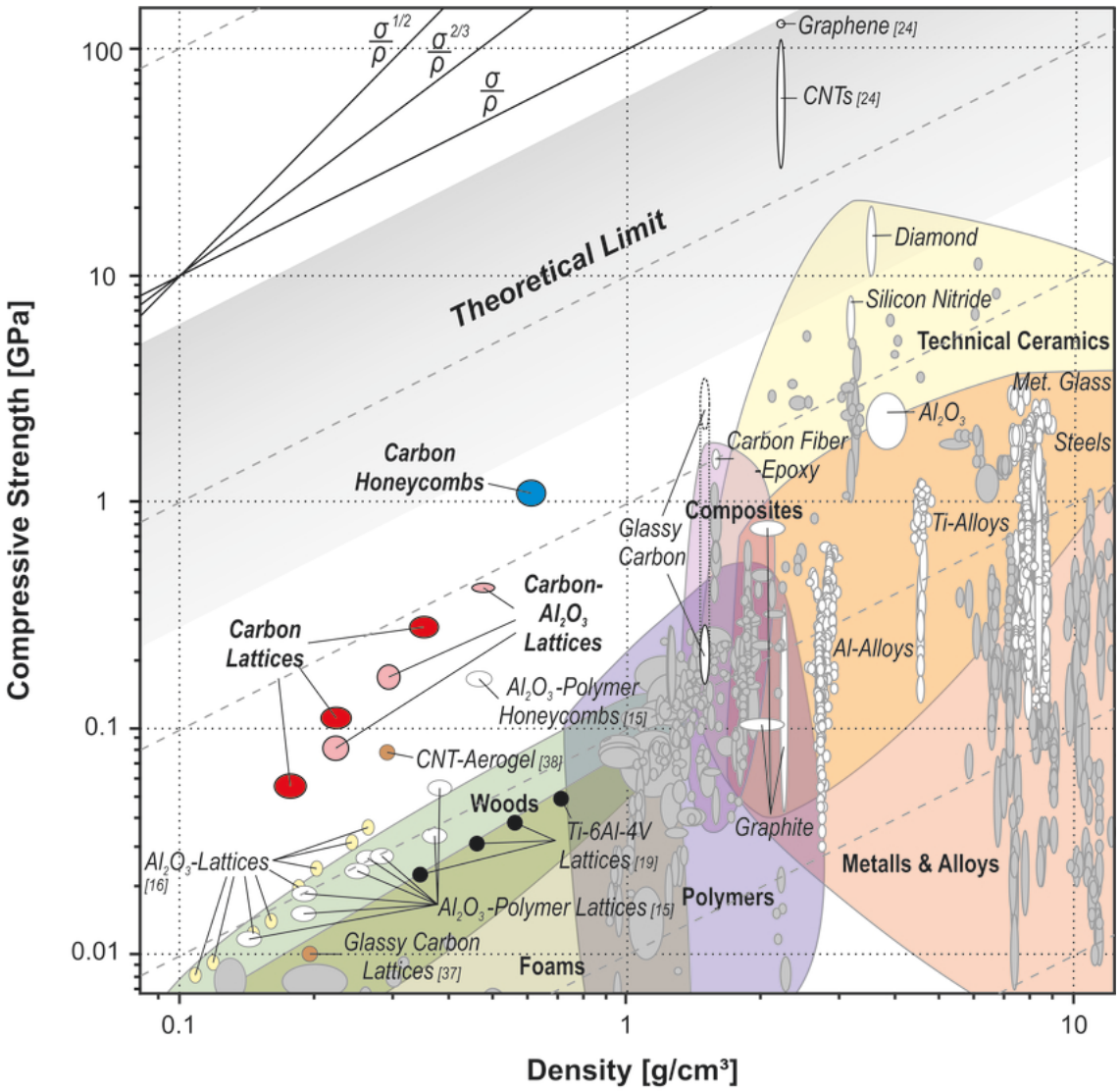

Figure 2: Compressive strength–density Ashby map. This chart compares the carbon and carbon–alumina lattices and honeycombs of this study against other architectured materials reported so far, natural and technical cellular solids, and monolithic bulk materials. Source: [10].

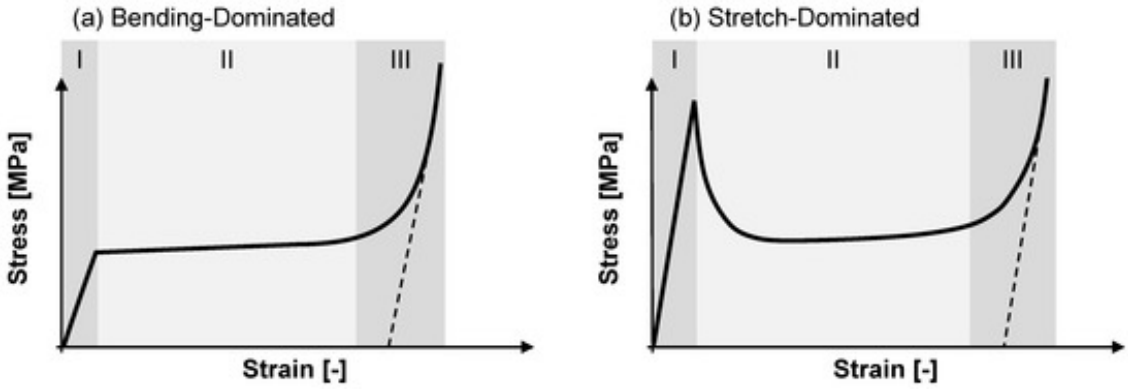

Figure 3: Stress-strain diagram of Bending-Dominated lattices vs. Strech-Dominated. Source: [6].

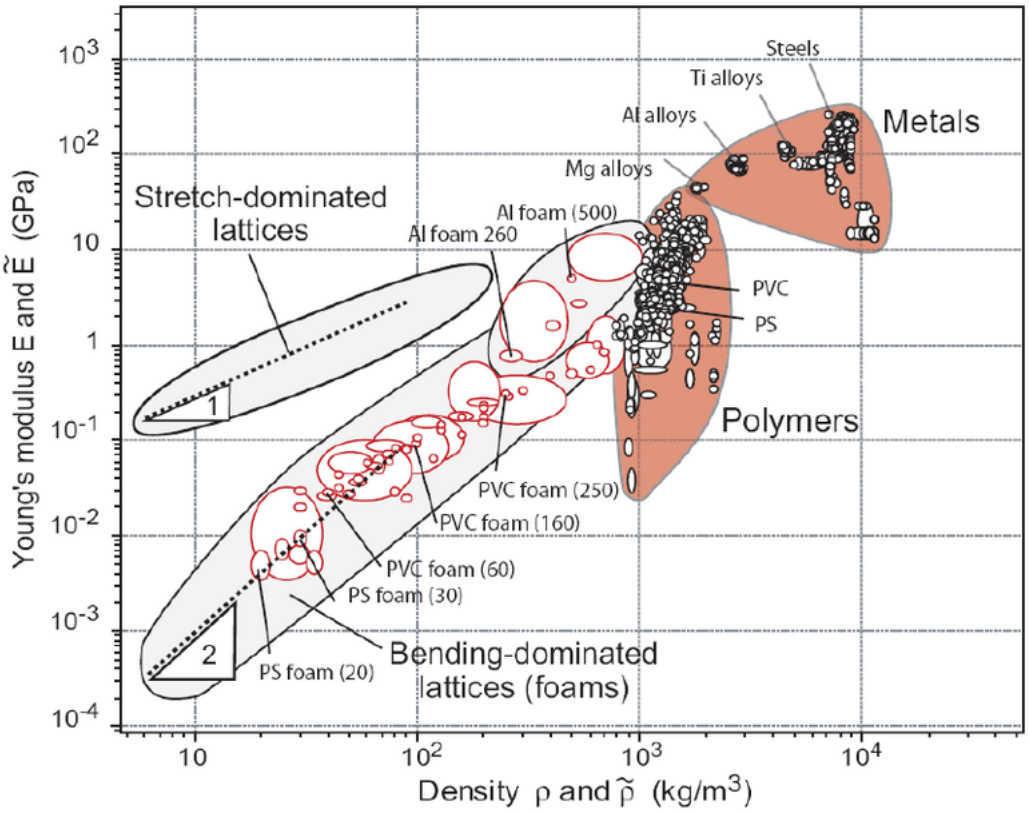

Figure 4: Ashby diagram. Source: [43].

Name of unit-cell	Deformation mode	Scheme
Tetrahedron	Stretching-dominated	
Hexahedron	Bending-dominated	
Dodecahedron	Bending-dominated	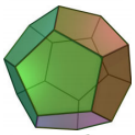
Rhombic dodecahedron [41]	Bending-dominated	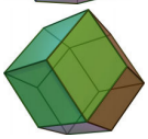
Icosahedron	Stretching-dominated	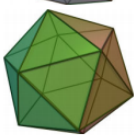
Tetrakaidecahedron [40]	Bending-dominated	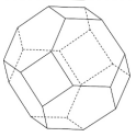
Simplest foam model [9]	Bending-dominated	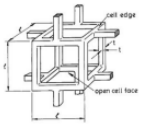
Octet-truss [42]	Stretching-dominated	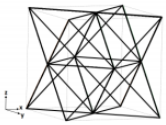

Figure 5: Examples of unit-cells with the deformation mode. Source: [41].

1.3 Aim and scope of the thesis

Nowadays, parametric design is becoming more popular. It is the paradigm based on the idea of describing the desired model, expressing it in terms of the design parameters and roles that relate the design variables with the design response. The thesis work aims to provide a parametric tool (software) for generation of lattice structures geometry in a computer. It is desired to make easier the study of the their response and verification of theoretical models on their behavior.

This thesis aims to provide a tool to study these fascinating structures in a simpler way. Attention will be mainly focused on speeding up the generation of the lattice structure CAD in a parametric design approach. We will present a Python package is willed to script. It aims to be computationally efficient and tries as well to take advantage of the geometrical properties of lattice structures. We will also present several examples where the package has been used for structural mechanics study purposes of such structures.

The main goal of the thesis is achieved in several steps. First of all, a research on lattice structures, definition and properties as an overview. Then, a revision on the actual available generative software which includes lattice structures generation and parametric tools for their design as well as analyzing their pros and cons to better understand the requirements of the software we aim to create. After these steps are done, the goal is to create a software able to generate lattice geometries in a computer and can compete with the available one in the market. Additionally, we see this work as a learning process not only as for programming but as a deep understanding on lattices topology in a more mathematical way. Consecutively, a verification of the software is needed and might be carried through testing. Finally, we want to show real applications of the software, giving several examples where it is used.

2 Literature review

2.1 Lattice structures

In this section we give an overview of lattice structures from their historical background to the current applications.

2.1.1 Historical background and inspiration

As mentioned, lattice structures have been known for generations but it was four decades ago it came across the understanding of materials with cellular structure. However, due to the difficulty of manufacture them limited their application . There were manufacturing processes which were capable of manufacturing lattice structures, but they were expensive and complicated [7]. Limitations cause that most of research actions were focused on stochastic or prismatic materials, which where manufactured with foaming solidification processes [20, 22]. Manufacturing stochastic foam metals were cheaper than manufacturing periodic lattice structures [1].

Artificial lattice were inspired from their presence in the earth (reference). Many materials contain lattice structure designs. Some of them are considered lightweight structures such as tubular or prismatic structures like a honeycomb or hexagonal lattice structures similar to the cellular structures of wood.

A honeycomb, figure 6a, is a prismatic lattice with hexagonal shape as pattern of repetition. Bees use this kind of lattice because of its efficiency for storing the honey. Reference [47] reported that "According to a widely spread hypothesis, the bees aim at economy: If, by some reason, the volume of a cell and the width of the whole layer are given, they try to use the minimum amount of wax per cell". The author proves that the hexagonal pattern of the honeycombs is indeed the most efficient bees can use.

Another example is the fibers' shape of wood, see figure 6b. The tubular cells of wood make the stiffness and strength to be dependant of their density and the direction, i.e. being an orthotropic material. Fibers are oriented to be stronger and support the bearing loads in the necessary manner. Also a similar example can be found in human bodies, through the bones fibres, see figure 6c. The inside structure of bones is adapted to the loads affecting the human skeleton in the every day life. Bone fibers are oriented in order to be stiff in the required directions, but at the same time, preserve as light as they are [41].

2.1.2 Definition

Lattice structures can be defined as a space-filling unit cells that continuously repeat along any direction of the space without leaving gap in between [25]. The pattern of repetition is commonly defined as unit cell which is considered as the object that repeats through the space [8]. Their topology appearance distinguish them so as to

be considered stochastic or periodic structures, we define them bellow. In literature, authors typically ignore stochastic lattice structures due to their random nature and instead, concentrating on periodic structures [25]. Others sources base the definition on truss or frame structures [7, 48], distinguishing them from prismatic lattice, polyhedron, foams, minimalistic surfaces, ... This work consider lattice cells to be configured with not only rod or beam structures but also surfaces and plates

(a) Honeycomb, hexagonal prism lattice

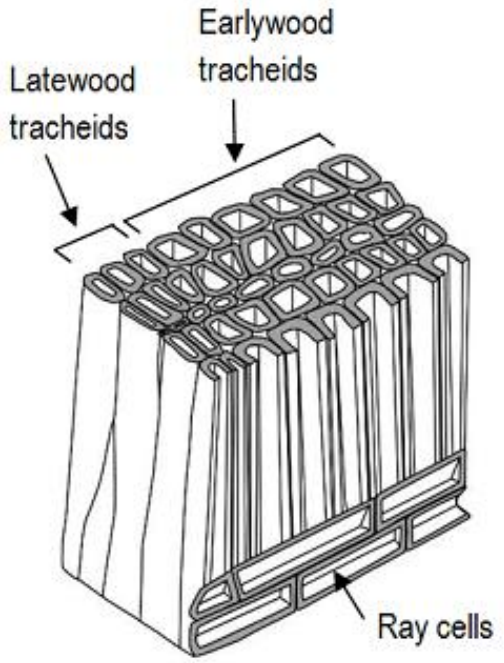

(b) Wood fibers

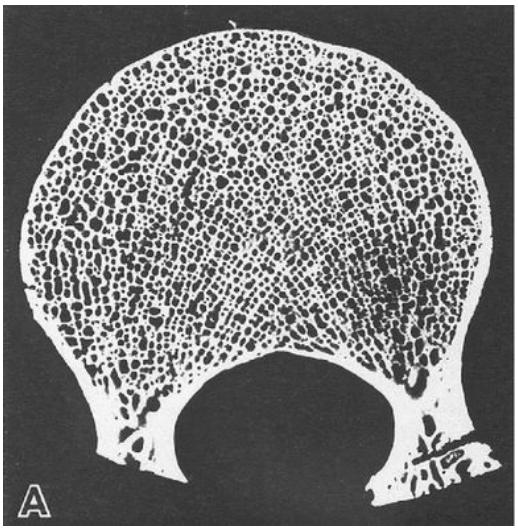

(c) Bone fibers

Figure 6: Examples of lattice structures in nature.

and volumes as in [25].

As we explained the classification of lattice structures is the following:

- **Stochastic** lattice structures are characterized by their arrangement of cells and shapes defined through a random probability distribution. Also, they are not characterized by having a non-constant unit cell dimensions. Examples of those kind of structures are bone structures, wood, cork, sponges, etc. Figure 7a, it shows a stochastic lattice structure modelled by a computer.
- **Periodic** lattice structures are created as functions of their inherent geometric properties such as cell dimensions, angle, quantity and final object boundaries [25]. Examples of periodic lattice structures in nature can be the honeycomb, the particles of a mineral which might form crystal structures, snowflakes which form fractals, etc. For instance, figures [7b to 7f] show five different periodic lattice structures.

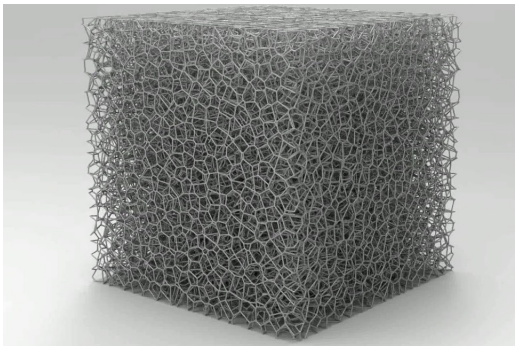

(a) Stochastic lattice structure. Source: [62].

(b) Periodic lattice structure, real AM examples. Source: [63].

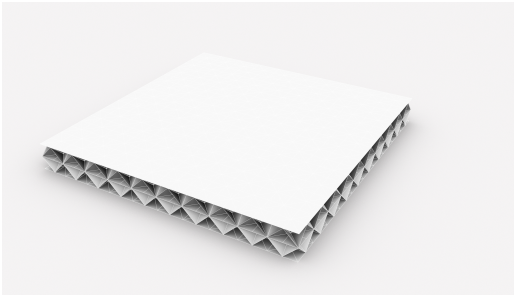

(c) Cuboid design space. Source: own (LNG).

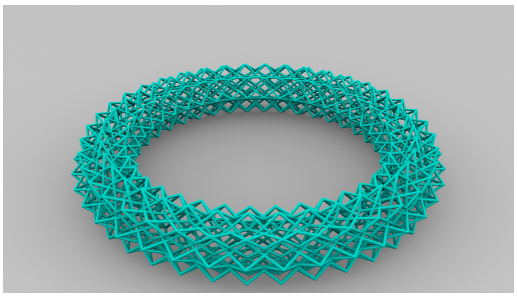

(d) Ring design space. Conformal lattice. Source: own (LNG).

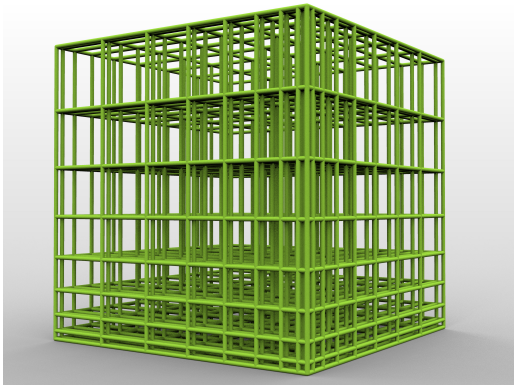

(e) Graded progressivity in all axis of periodicity. Source: own (LNG).

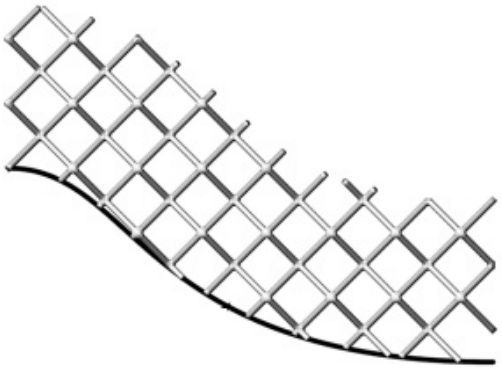

(f) Non-conformal lattice structure, real AM examples. Source: [15].

Figure 7: Examples of lattice structures.

2.1.3 Parameters

We consider six main variables concerning lattice geometries and inspired by reference [7] and [4]:

- The lattice **pattern** is the basic element which is repeated creating the lattice structure. It is based on nodes positions and edges connection between these nodes and, as mentioned before, they can be configured with surfaces and volumes. There are many types of lattice structure patterns. We divide them into 2D patterns (their nodes are co-planar) and 3D patterns. An example of 2D patterns is shown in figure 8.
- The **design space** is defined by the structure domain extension. In other words is the volume enclosing the lattice structure. Examples include simple 3D cuboids, representing beams, to complex volumes, as it can be the shell bonnet of a car or the sole of a sport shoe.
- **Axis of periodicity** are those directions in which the pattern is repeated. Note that the maximum axis of repetitions that a lattice can have are three if it is defined in a 3D design space. They should not be confused with the symmetry axis that can appear in a geometry due to intrinsic symmetric properties of the pattern.
- Lattice **relative density** is defined as the ratio between the volume of the lattice structure and the volume of the design space.
- Lattice **progressivity** relates with the pattern repetition through the space and the cell-size. Periodic lattices have specific axes of repetition in the space. Then, the periodicity can follow different functions. For instance a lattice structure can have constant progressitvity, so that the cell-size is uniform through the axis of periodicity. But the cell-size can also be gradient and constantly grow along the axis. Going even further, other options would include follow, for example, trigonometric functions so that the cell-size is continuously growing and diminishing along the axis of periodicity. Nevertheless, stochastic lattices have indeed random progressivity in random directions. An example is showed in figure 7e
- Lattice **conformality** relates the axis of periodicity with the design space. When lattice axis are aligned with the boundary domain, the lattice is considered to be **conformal** e.i. figure 7d. Otherwise, the lattice is considered as **non-conformal** as figure7f.

2.1.4 An overview of applications

Lattice structures are widely exploited throughout various fields. Some of their applications are the following:

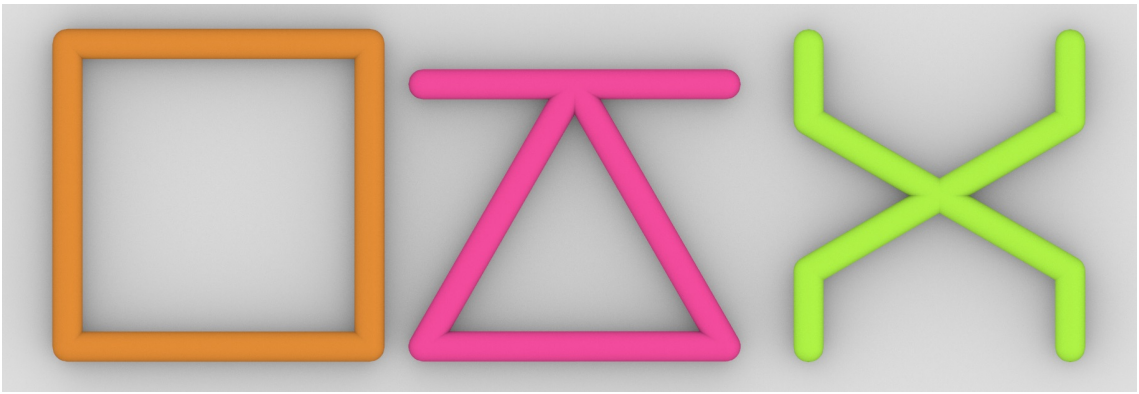

Figure 8: Unit cell examples in 2D, plane.

- Lattice structures are used for parametric design as in **civil engineering** or in **architecture**. In civil engineering projects they are commonly used for their ability to bear loads and withstand large stresses due to modifications in the configuration of the inner structure. They can be arranged to carry loads in the most efficient way. Hence, a reduction on energy and material can be achieved with their utilization. Moreover, they are also utilized for their aesthetic properties.

- In the field of **material science**, they are being used in **architectural micro-structured materials** of different scales: from macro to micro and nano. They are created at those scales being able to obtain low dense materials that at the same time maintain their strength in the desired directions. In **automotive** and **aerospace industries**, the weight is a critical parameter for the efficiency of the vehicles. Mass reduction in vehicles structures improves their performance and therefore, it has been a constant and relevant challenge in the space and industrial business [14]. With lattice structures it is possible to rise the efficiency of the vehicles by proportioning high stiffness to weight ratio materials.

- In **medical industry**, the ability of maximization of surface areas, lattice structures can be particularly useful in the characterization and production of scaffolds optimized for tissue and bone replacement in order to encourage osseo-integration [13]. There has also been research put into the accurate recreation of cancellous and cortical bone structures through the variation of density scaling parameters, in particular optimizing characterization and modelling for additive manufacturing [16]. Their ability to minimize material requirements during implantation notoriously decrease invasiveness and recovery time.

- Another interdisciplinary property is lattice **energy-absorption**. As the lattice structures are able to propagate energy through themselves, they are very useful in distributing an impact shock across the object and therefore serve as a protection [18, 33]. **Auxetic lattice structures** which posses negative Poisson's ratios are particularly useful in absorbing energy. For instance in footwear, auxetic designs of soles leads to create those which expand in size while walking or running, thus increasing flexibility. For instance, one of the key solutions for reducing **noise pollution reduction** by increasing damping capacity and optimizing pore structure of materials such as lattice foams [60]. Sound waves absorption effectively through internal vibration and frictional loss of the sound waves in the cellular structure The most important characteristic of flexible polyurethane foam is to have cavities with interconnecting open pores, and its cell structure can play a crucial role in controlling not only mechanical but also acoustic properties [66].

2.2 Review on software

This subsection is devoted to the existing computer tools providing lattice geometry creation. It should be mentioned that there is actually a small amount of software aimed at the design and study of lattice structures on actual available tools providing lattice geometry creation. There are actually a small amount of software aid in design and study of lattice structures. Descriptions given in the current subsection are based on the publicity available information. The common pros and cons of these tools are summarized based on the idea of utilizing them for research purposes.

2.2.1 Software report

STL Lattice Generator
STL Lattice Generator© is a simple program written in MATLAB that generates lattice geometries and then it can easily be convert it to STL format. The program is created by Marten Jurg (RMIT University). The author present the program to be "for a fast and simple way to generate STL lattice structures for research purposes". It incorporates several lattice patterns for creating cuboid lattice structures. Moreover, the author explains that "in theory, any lattice configuration could be added". Additionally, the software incorporates a function for generating FE meshes in NASTRAN format, however it is not having any feature for FEA. STL Lattice Generator© is open-source but it demands MATLAB software which is not a free. The main weakness is that the autor have not upload any documentation of the scripts and functions it incorporates so users have to base their scripts on the examples found in the program web page. (`https://www.mathworks.com/matlabcentral/fileexchange/48373-stl-lattice-generator`)

Netfabb
Netfabb® is a software from Autodesk. It can fill 3D volumes from a predefined unit lattice cells and generate lattice structures. In the last release, they included simulations and topology optimization modules. However, the software seems to not include many features for the FEA and post-processing. Nevertheless, it is not a free software. (`https://www.autodesk.com/education/free-software/netfabb-premium`)

Element
Element® is a software from the company nTopology. Similar to Netfabb® , it is a design software to generate lattice structures inside volumes or surfaces of design models. It integrates FEA for topology optimization. The company present different versions and prices of the software based on the features Element incorporates. There is one free version of the software, Element Free® , but important limitations are that neither "import" and "export" options nor post-processing tools are available in this "free" version. (`https://ntopology.com/`)

Within
Within® is a software from Autodesk. This is a professional software divided into

Within® and Within Medical® packages for industrial and medical engineering purposes, respectively. It is a quite compact program offering the same features as Element Pro® and even more regarding lattice structure configurations. Nevertheless it is not a free software. (`https://www.asidek.en/fabricacion-aditiva/autodesk-within/`)

Materialise Magics
Also in the same line as Element Pro® and Within®, Materialise Magics® offer a generative design option. It is developed by Materialise company which at the same time offers other programs for topology otpimization, product management, etc, related with 3D printing. All the packages they offer are priced and they are apparently developed for companies. (`https://www.materialise.com/en/software/3-matic/modules/lattice-module`)

Intralattice
Intralattice© is a plugin for Grasshopper® (parametric design package) used to generate solid lattice structures within a 3D design space. It is developed as open-source software and it is shared in GitHub.. However, Grasshopper® and Rhino® are required so it is limited to their users, these last softwares are not free. Intralattice© was developed at McGill's Additive Design and Manufacturing Laboratory (ADML). It includes manifold options of lattice structures, nevertheless, in some cases its Grashopper® model, its user-interface, is not easy to build and not even intuitive. (`http://intralattice.com/`)

Crystalion
Crystalion© is a plugin for Grasshopper as well in the same purpose as Intralattice©and mostly with the same features. It is also developed as open-source software, available in GitHub. It was developed at FATHOM by Aaron Porterfield. (`https://studiofathom.com/blog/introducing-crystallon`)

2.2.2 Pros and cons of the current software

In general, the present software tools are useful for design of lattice structures. They all have the capability of creating lattices with different cell patterns. It is not clear if they can build conformal lattice based on the design models. Some of them include FEA modules to evaluate the design structures under static structural loads. These modules are usually a "black-box", neither a clarification is given about the Finite Elements modelling the objects nor about the FE approaches utilized. Moreover, three of them include optimization tools to create light-weight designs but methodologies are not documented. Almost all of them present a graphical user interface, GUI, and are created to be user friendly, limiting the customization of their built-in functions and other design parameters. Also, the majority are not open-source packages and they are intended for commercial use.

3 A tool for generating lattice structures geometry

This section describes the tool that has been developed as a part of the thesis. First, we start by describing the tool and its scope. Afterwords, we go further into details of the geometric problems that have been studied in order to make it efficient in a computational point of view. Then we explain the working structure and back-end engine. To conclude this section, we present the features it is incorporating and we briefly describe the main advantages that the tool brings compared to the already existing software. We finalize by describing possible improvements and newer features that can be implemented in future versions.

3.1 Introduction to Lattice Net Generator

As we exposed there is an absence of functional open-source software that enables parametric analysis of lattice structures as well as handy integration of FEA. This tool has been arisen due to the need of study and design lattice structures.

The package allows generation of periodic lattice structures by their geometric data described in a parametric way. The tool has been named Lattice Net Generator, LNG. LNG is written in Python™_and requires the following Python™existing packages: `numpy`, `math`, `dxfwrite`, `pylab`, `scipy`, `copy` and `matplotlib` and `mpl_tolkits` for visualizing the data.

LNG primary goal is to serve as an easy accessible tool that can be modified to explore and study lattice structures. However, its function is not limited to creation of lattice structure geometries. The arrangement and configuration of the encoded mathematical description of such geometries grant a broad of possibilities. The data generated is always controlled and stored with simple structures so that it could be exported to any kind of data file.

LNG includes basically two main classes: one refers to the RVE description and the other refers to the lattice structure topological and geometrical data. RVE class creates an object which stores the data related to the basic element that will describe the lattice structure, the pattern or RVE. An important appeal of this class is that it leads to chose an RVE already stored e.g. a triangular-truss, an octet-truss, etc. But there is also the option of defining a new RVE and customize it. From the other hand, the second class stores the hole lattice structure in an object. It contains a method that generates the lattice structure data from the RVE class. Besides those two classes other functions offer the possibility to export the geometrical data as "dxf" file, to refine the mesh of the structure, to visualize the objects created by LNG and other auxiliary functions.

3.2 Adapting graph theory on the algorithm of LNG

Lattice structures are geometric objects that can be defined as graphs. Conceptually, in graph theory, a graph is formed by nodes (also named vertices) and edges connecting the nodes. When edges create a cycle then this is called to be a face, i.e. a polygon. A set of faces is called surface.

The following mathematical statements are important for defining lattice graphs:

Statement 1, [53]:
"Lattice structures are geometric objects that can be defined as a graph. A lattice graph, also named as a mesh graph or grid graph, is a graph possessing a drawing whose embedding in a Euclidean space $\mathbb{R}^n$ forms a regular tiling."

Statement 2, [54]:
"A tiling is a collection of disjoint open sets, the closures of which cover the plane. Given a single tile, the so-called first corona is the set of all tiles that have a common boundary point with the tile."

Statement 3, [54]:
"Wang's conjecture (1961) stated that if a set of tiles tiled the plane, then they could always be arranged to do so periodically."

Therefore, following graph theory we define the data structure that is created by LNG in the following manner:

- **Nodes, defined with a coordinates array**: Nodes, or vertices, are the primary elements that define the lattice geometry. They bring the spatial information with coordinates. Coordinates are stored in an array where each row corresponds to a different vertex of the graph. The row indexes of the array relates to different vertex, they give the correspondent unique identifier to each node of the lattice structure.

- **Edges, defined as an adjacency list**: Edges are defined as connections between nodes in the lattice graph, they can be directed or undirected, which give also the property to the graph as directed or undirected graph. For simplification, we consider the undirected graph. Edges are classically stored in three different ways: edge list, adjacency list or adjacency matrix. An edge list stores, row by row, the nodes connected by each edge. The adjacency list contains as many rows as nodes in the graph; each row corresponds to one node and contains a list with the nodes connected to the row node. Adjacency matrix are square matrices as big as the number of nodes. They contain the number of edges connecting the nodes respective to the row and column index. We first discard the edge list because even they are easy to iterate over, most searching algorithms are so complex to apply on it. The option of choosing an adjacency matrix is also discarded. They are useful when they are dense

(almost complete graphs), when each node is connected to a large amount of nodes. Otherwise, they waste space which is not necessary but also they are expensive to iterate. A lattice graph is always far from being a complete graph, thus, the adjacency matrix would be sparse. Hence, we consider that a lattice graph might be stored in an adjacency list due to the fact that the number of connections in a node is always a very small number compared to the total number of nodes.

- **Faces, defined as a list of lists**: Faces are defined as objects bounded by a closed set of edges. They can be stored in many ways, however, they depend on the structure the edges are stored. In LNG they are stored as a list which contains sub-lists with the set of nodes surrounding the face. We chose this option because of the easy transmission of information to data files, which usually describe faces by their nodes. For the same reason, faces are limited to be defined with three or four nodes only.

- **Volumes, defined as a list of lists**: Although volumes are not implemented in LNG yet, they may be stored as a list containing sub-lists with the faces (with IDs as the faces list) which enclose the volume. Then, each list contains a closed set of faces that bounds the volume. Then, since in many cases it is desired to model the lattice with FEM, this structure would already contain the domain tessellated.

Based on these definitions, we build the LNG model to generate lattice structures with the following general idea. First, we describe the RVE pattern by its nodes, edge connections and face list. We call these properties to be local because their information is always referred to the node identifiers of the RVE. Next step is to reproduce this object through the space by applying transformations to the node coordinates, creating what we denote the global grid of points. Then, to transfer the local properties (edge connections and face connections) to the new objects, we make use of a transformation matrix that maps the local information to the global graph. This matrix works as the assembly matrix used in FEM. Each row refers to different lattice cells (RVE repetitions) of the global graph and each column relates global nodes to local nodes. Then, the matrix is always as large as the number of the lattices, times the number of nodes of the lattice RVE. Finally, we end up with the global graph that we call lattice structure. Note that the transformations we apply to the local nodal coordinates, in each cell repetition, will define the global shape of the lattice. According to this description, LNG builds the lattice structure following a lattice graph which intrinsically limits lattice structures to conformal.

3.3 LNG package

LNG contains several modules including the `builder`, the `main` and the `engine`. By executing the `builder` module, it automatically calls the others to generate the lattice structure resulting in a class. Then, "main" module contain the class object definitions of `RVE` and `LatticeStructure`. Most of the methods included in these

classes require functions that are defined in the `engine`.

The inputs of the LNG `builder` are based on the required ones for creating a `LatticeStructure` class, which include the RVE class inside. These inputs are indeed related to the parameters explained in section 2.1.3 and are exposed in figure 9. Regarding the RVE the inputs, they are the identifier of the element type already stored inside LNG and the size of the RVE (the dimensions of the box enclosing the RVE, also called cell size). Then, the inputs related to the lattice structure itself are: the shape of the global structure and the density of RVEs per each axis of the lattice. The shape can be chosen from those already stored in LNG, but it is possible to create new shapes as well. The density of RVE, denoted as "n_G", can be defined as the number of RVE repetitions in each periodicity axis the lattice is extended... Once one execute the `builder` lattice structure topological information is structured in arrays and lists and stored as attributes of the `LatticeStructure` class (class attributes can be understood as the object properties).

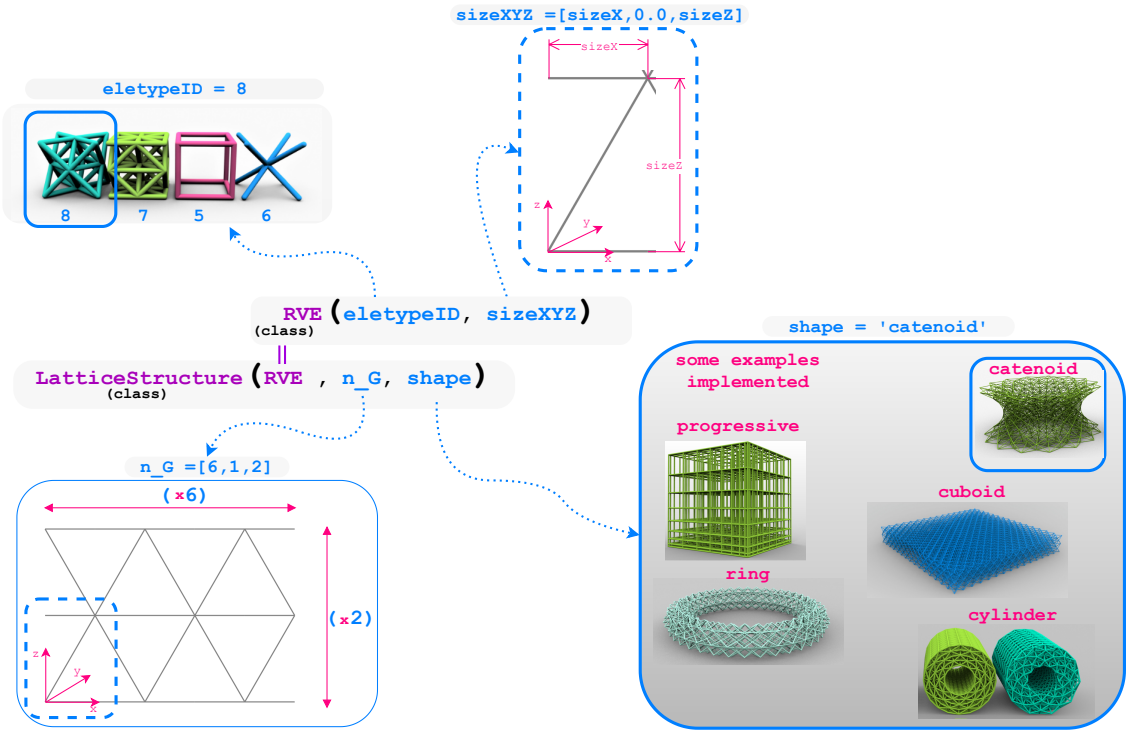

Figure 9: Inputs required to create a lattice structure with LNG.

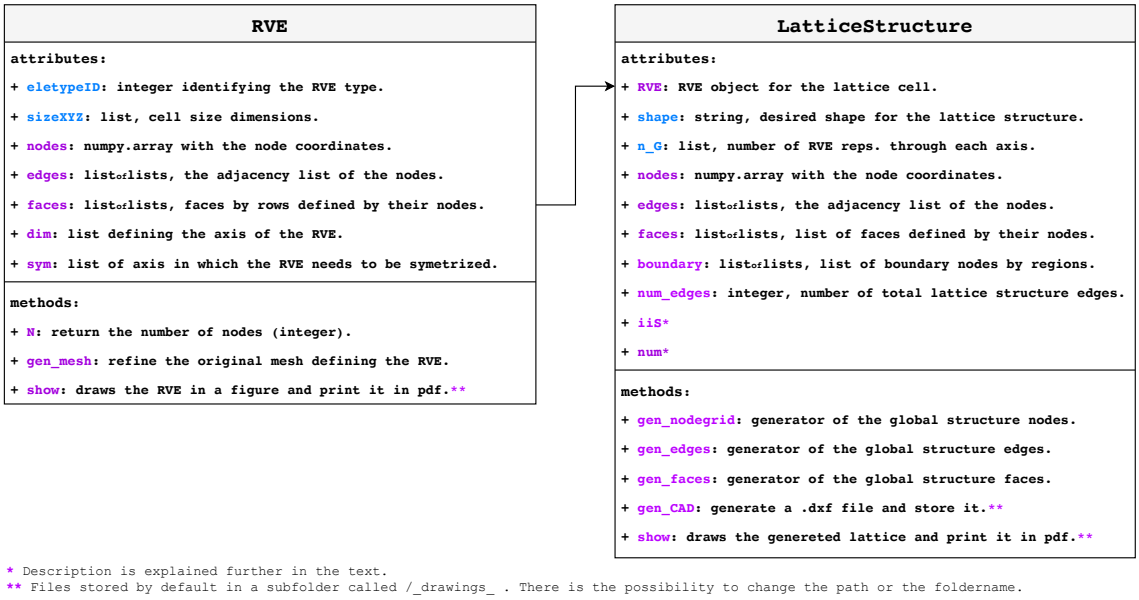

Figure 10: Summary of RVE and LatticeStructure objects attributes and methods.

3.4 Complexity

An important goal of the designed code has been the efficiency in terms of the computational cost which is reflected on its time and space complexity. Naturally, the performance of the algorithm depends on the number of nodes of the lattice structure, n, the number of edges, m, and the number of faces, l.

The LNG `builder` has a time complexity of $\mathcal{O}(n)$, $\mathcal{O}(m)$ and $\mathcal{O}(l)$ due to the fact that the algorithm is only iterating once over each of those elements to create the lattice structure. The following graph 11. The graph shows the number elements vs. the time the LNG takes to build the lattice. Note that they are normalized with the maximum value of each axis data. The axis are in logarithmic scale, hence, since the slope of the curve is, in average, 1.0 it means the relation between the axis is linear. The space complexity is also $\mathcal{O}(n)$ and it is proved simply with the data structures where LNG stores the geometrical information. Even that one should take into account data stored meanwhile the algorithm is running. We ensure that this data is not increasing the final space complexity.

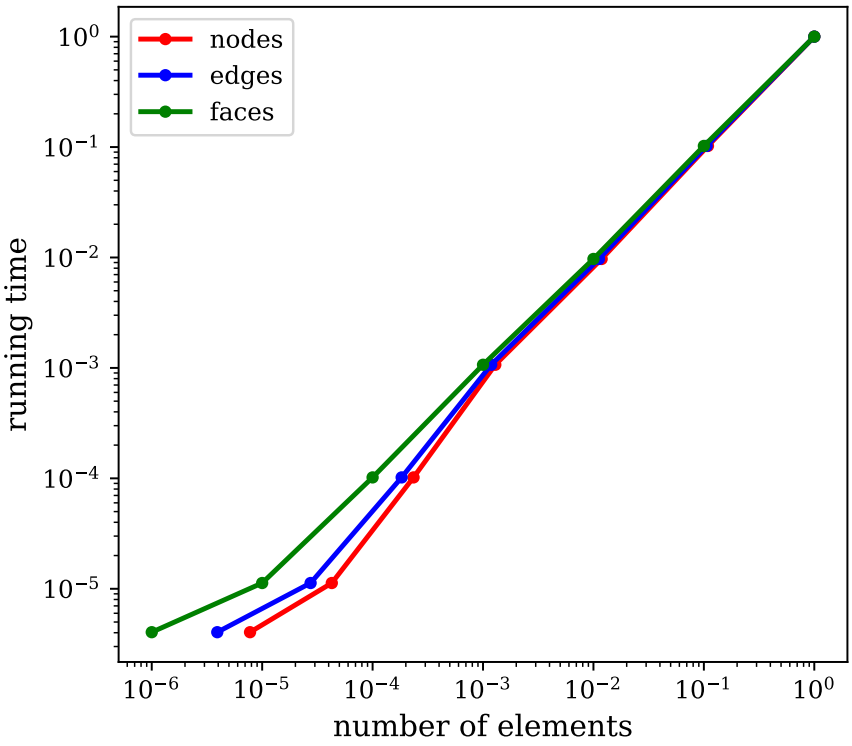

Figure 11: Time complexity analysis of LNG. Source: own.

3.5 Features of the LNG

Here we present the main features of LNG:

- **RVE pattern customization**: Possibility to create any RVE as long as the nodes, the edge list and the face list is given (if the RVE contains faces). LNG includes already several predefined RVE in 2D (the nodes are co-planar) and 3D (more than 10). See figures 8, 2D RVE, and figures 12 and 16, 3D RVE. Note that the 2D RVE can only create lattices structures which will create a surface reduced in a 2D space, prismatic structures are not implemented yet. Therefore, they can only be periodic in two dimensions, i.e. the lattice shape would be seen as a surface.

- **Design space, conformality and periodicity axis**: LNG is only capable to define conformal lattice structures. Therefore, the boundary of the lattice is always aligned with the axis of periodicity. Angles between edges of the lattice are conserved from the RVE definition to the conformal global space of the lattice shape. LNG can reproduce any lattice shape which can be parametrically defined, see figures 1415.

- **Progressivity**: Both constant and quadratic progressivity is implemented.

- Create **random** irregularities in the mesh following a probability distribution. These irregularities can be on the coordinates of nodes or also erasing edges of the global grid. The parameters and the type of distribution can be customized. See Figure 13.

- **Meshing**: Possibility to generate the mesh of the domain (except of 3D volume). The mesh is defined with the minimum and maximum size of the edges/struts connections.

- **Boundary control**: LNG store the boundary nodes of the lattice structure at the same time it creates them. This saves a lot of computational time by avoiding posterior nodal searches to apply the problem boundary conditions. Each set of boundary nodes is saved as a list in `LatticeStructure` class after it is created.

- **.DXF extraction**: Optional extraction of the geometry data to .dxf file. Edges and faces are stored (redundantly) in a layer called "edges" and another called "faces", of the .dxf file.

- **Visualization**: Even that we have commented that the visualization of the geometry is computationally expensive, we have add the option to export a simple 2D or 3D plot to visualize the lattice geometry at the same time the lattice is created. This is a small feature made to easily check the lattice structure correctness.

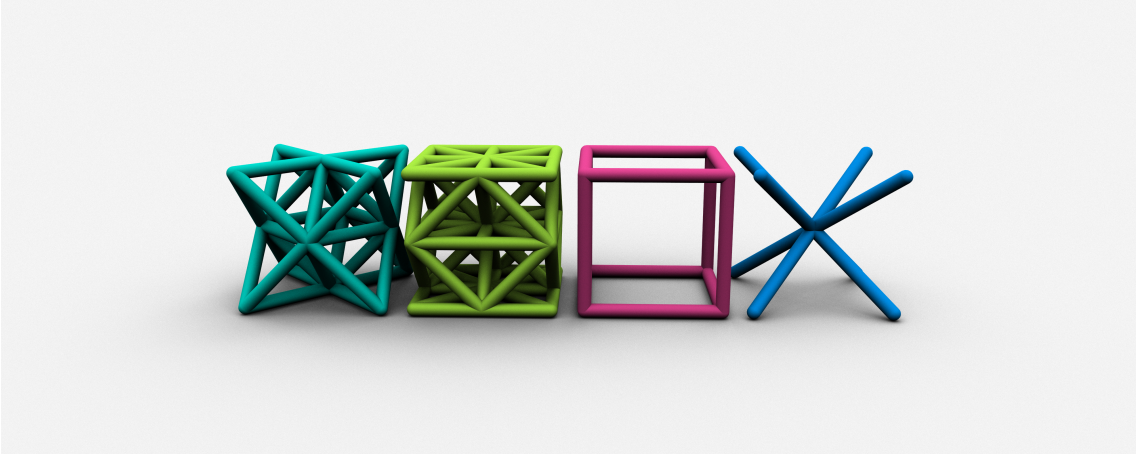

Figure 12: Examples of possible patterns in 3D. From left to right: octet-truss, hexa-tetrahedron, cube, X-cross. Source: own.

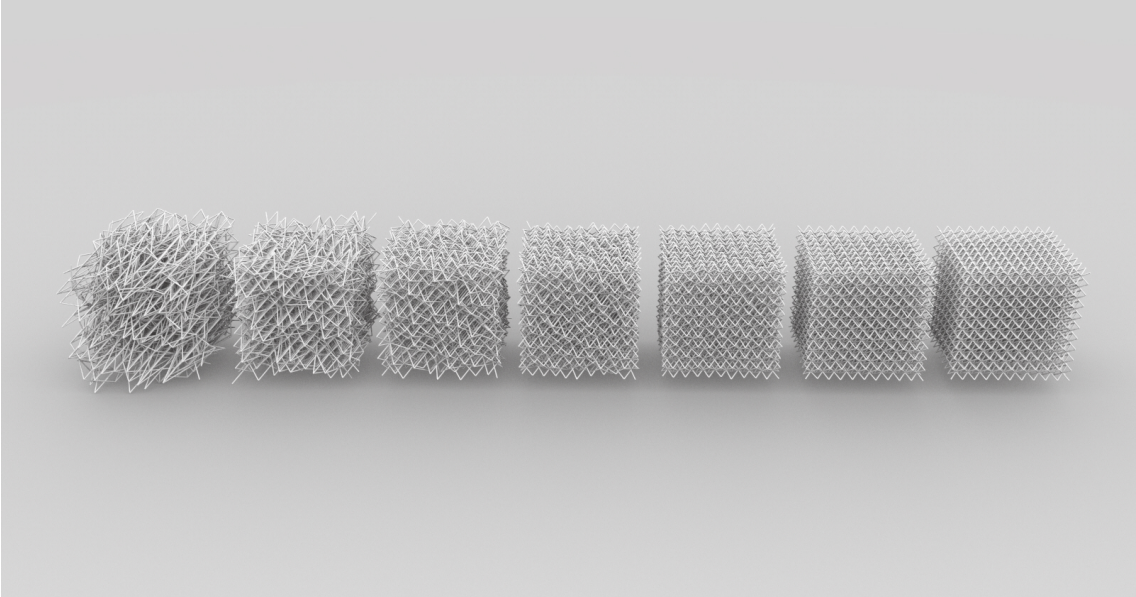

Figure 13: Introduction of random irregularities. Degree of irregularity increases from right to left. Source: own.

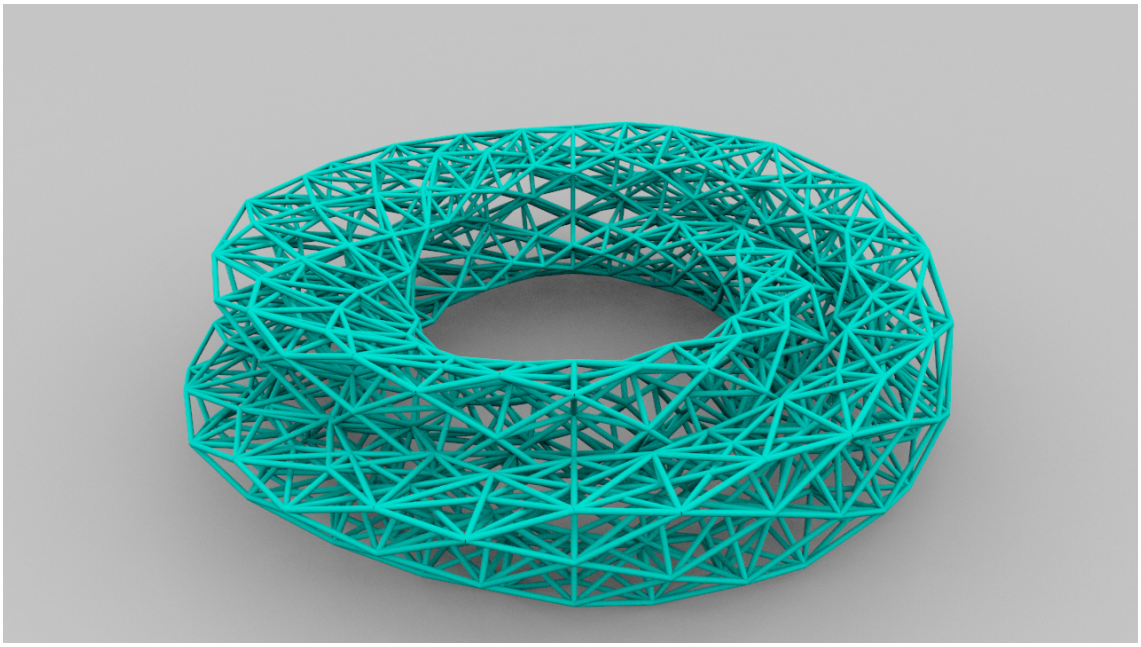

Figure 14: Klein bottle lattice. Source: own (LNG).

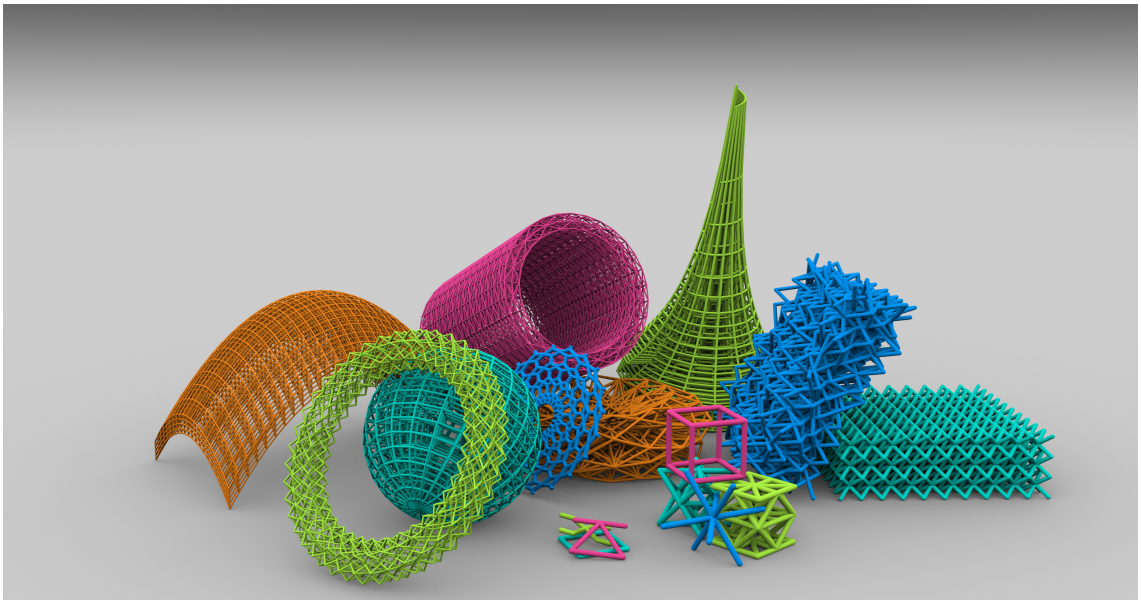

Figure 15: Multiple examples of design spaces. Source: own (LNG).

3.6 Advantages and future improvements

For the moment, we have shown what LNG is capable to create. The most relevant feature of the package is that the structure in which it is build allows any customization. For instance, we add the randomness option, as explained before, to introduce deviations to the lattice structure, which is a feature that is not included in any other software. Another important point is that it can be easily integrated to any other package, e.g. to perform FEA simulations, due to the simple data structures

it contains. Next chapter present some examples in which we integrate it in FEA. Moreover, it can not be missed the advantage of obtaining the boundary nodes at the same time that the structure is created. Last but not less, it brings the meshing function which speed up the FE pre-process.

On the other hand, although the first release of LNG brings a lot of possibilities for generation of lattice structures, there are still a lot of features that can be included to it. We list the capabilities we would like to add to LNG:

- Volume handling. LNG is not able to recognize volumes. However, one can create sets of surfaces that enclose a volume but in case of exporting the data to a .dxf, it will not recognize it as a volume.
- Non-conformal lattices. It would be a good extension in order to study their performance compared to the conformal ones.
- Automatic piping of the edges. Usually truss-lattices are created with rots which physically have a shape of a pipeline. Some software is already including this option, but there are still a lot of debate on how to adapt it to lattices, specially for the nodal zones.
- Export in other formats. Sometimes .dxf is not the best format for transferring the geometry data. We would like to add .stl exporting and others to make the data easily interchangeable between other programs.
- Importing geometry. For the moment LNG is not capable to read geometry files. It would be a good option to be able to do so.
- Own integration of FEA. We would like to add FEA into LNG package without requiring external packages to be able to adapt it on line with the study of lattice structures and its properties.
- Triply periodic minimal surface lattice structures. We have not found specifications on the available software if it is handling this kind of lattices. For this reason, it would be interesting that LNG has the capability.

Finally, we want to add that LNG is currently in GitHub in the following web address: `https://github.com/criscapdechoy/LNG`. For the moment, we do not allow "pull requests" (other user changes) but it can be clone (downloaded) for everyone.

4 Examples

The objective of this section is to show the applicability of LNG and its advantages for modeling and analyzing lattice structures. We present study cases in which LNG speed up the parametric analysis of lattice structures. Moreover, in order to expedite the tests we have included the FEA as a scripting part, as an alternative to the non-scripting software.

The scripted FEA has been implemented with Python package, named Openseespy. However, we additionally use COMSOL Multiphysics©to verify each scripted routine by comparing the FEA solutions. In some cases, we have also employ it for post-processing the data and visualize the samples.

First example is a lattice plate bearing an edge load, it is tested for different RVEs configurations. Then we repeat the test as a second example but we model different cylinder lattice structures under self weight. We proceed with the third example that consist on introducing defects on one of the previous cylinders, using octet-truss RVE. In this case, we aim to approach the error on the structure behaviour due to geometrical defects as missing lattice beams. In the fourth and fifth examples, we study the global structure effects related with the internal lattice structure density, commonly known as size effects. In these tests, we model a rectangular cross-section beam in a 2D plane and a rectangular plate in a 3D space respectively with a free-edge point load. The goal is to give an estimation on the effective mechanical parameters of the given structures following the gradient elasticity theory. Finally, we just model an octet-truss plate with an intention of observing size effects.

4.1 Comparing cantilever plates made of different lattice RVEs

As a first example, we show how LNG can be utilized to analyze different typer of RVE lattice on determined lattice structure. We start by creating a quadrangular lattice plate (side length = L and height = h) with different RVE patterns. Consecutively, we build the FEA model by applying the following boundary conditions: we fix one of the edges ($X = 0$) clamping the nodes and we load the opposite edge with an edge-load, F, on $X = L$ boundary nodes.

Figure 16 shows the lattice RVEs we have chosen for this first example. From the left to the right they are an octet-truss (turquoise), an FCC (green), a CFCC (dark blue) and an hexa-pyramid (pink) [75]. The cell size we utilize to build the RVE is ($2.0\,\text{mm} \times 2.0\,\text{mm} \times 2.0\,\text{mm}$) in X, Y and Z direction respectively. The quantity of RVEs we use in each direction to create each sample plate is $(n_X, n_Y, n_Z) = (15, 15, 3)$ where nX, nY and nZ are the number of RVEs per axis. Therefore, the lattice plate size is ($60.0\,\text{mm} \times 60.0\,\text{mm} \times 6.0\,\text{mm}$) i.e. $L = 30.0\,\text{mm}$ and $h = 6.0\,\text{mm}$.

The last parameter is the cross-section geometry for the lattice beams. We

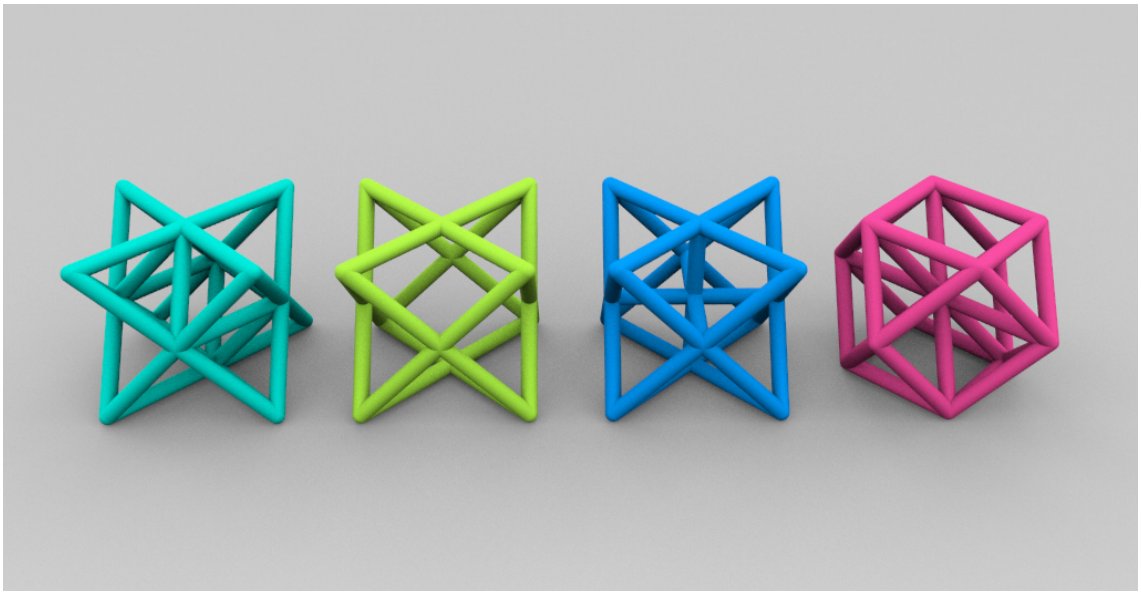

Figure 16: Lattice RVEs used for example 1. Source: own (LNG).

consider a quadrangular cross section with side size a. Then, we define a for each sample so as to keep the overall lattice volume constant. Note, that we approximate these volume as $(l_e - n) \cdot a^2$. Where l_e is summed length of all lattice beams and n stands for the number of nodes. Table 1 shows a values for each sample and the material parameters we have chosen for the structure. Finally, we execute the FEA using Openseespy package and we get the resulting edge displacements at $X = L$, table 1. Figures A2a-A2f show the resulting Von Misses stress in the hexa-pyramid lattice plate. Please refer to Appendix A, figure 17, which includes the stress 3D plots for the four cases, generated with COMSOL.

Table 1: Plate samples data.

Material data		
Young's modulus		2×10^9 Pa
Poisson's ratio		0.25
Density		$1040\,\mathrm{Kg\,m^{-3}}$
Cross-section data, a		
Case	Pattern	Side length, a m
1	Octet-truss	1.00×10^{-1} mm
2	FCC	1.47×10^{-1} mm
3	CFCC	1.27×10^{-1} mm
4	hexa-pyramid	1.00×10^{-1} mm

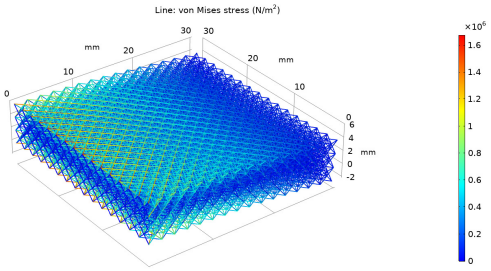

(a) Case 1, perspective view

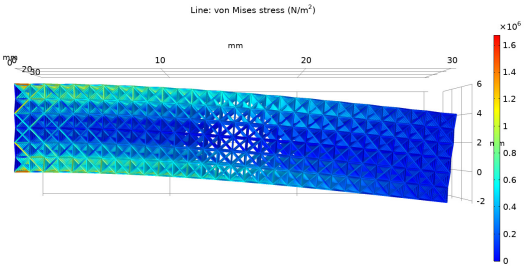

(b) Case 1, lateral view

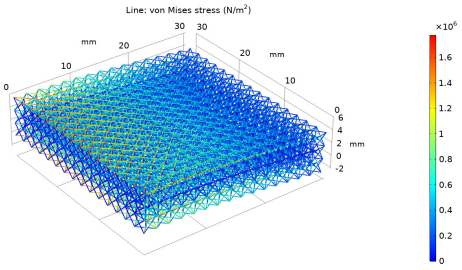

(c) Case 3, perspective view

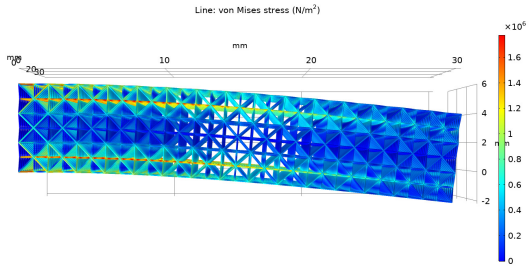

(d) Case 3, lateral view

Figure 17: Resulting Von Misses stress state of two different lattice plates. Sub-figure a) and b) correspond to the octet-truss and figure c) and d) correspond to the CFCC pattern.

Table 2: Mean nodal displacement at the free edge, $x = L$.

Case	Pattern	Displacement (-Z axis)
1	Octet-truss	1.402×10^{-1} mm
2	FCC	1.060×10^{-1} mm
3	CFCC	9.333×10^{-1} mm
4	Hexa-pyramid	1.392×10^{-1} mm

From figure 17 and A2 we can estimate how the RVE's configuration affects on the lattice structure behaviour. One can see that the appearance of Von Misses stress field through the global plate domain is distributed following different schemes for case 1 than for case 3. Finally, from table 4 one can see that each case presents different mean nodal displacement (mean value of the displacement at the edge nodes, $X = L$). Note that case 2 and 3 are being stiffer than case 1 and 4 regarding that the volume of the lattices is the same. Please note that Appendix A, figure 17, includes the stress plots of the four cases.

Finally, we would like to expose that different RVE configurations leads different behaviour in bending. Hence, we obtain different deflections and absolutely different stress fields. This is an example of a parametric study: from it we can conclude that FCC-lattice is the most effective (less deflection). Regarding the stress distribution, we see line concentrations in CFCC pattern and more homogeneous distribution on the others.

4.2 Comparing cantilever hollow-cylinders made of different lattice RVEs

In second example, we experiment with a lattice shell. We model a lattice hollow cylinder which is clamped at one edge and free at the other. The loading condition we apply is the gravity load i.e. self weight.

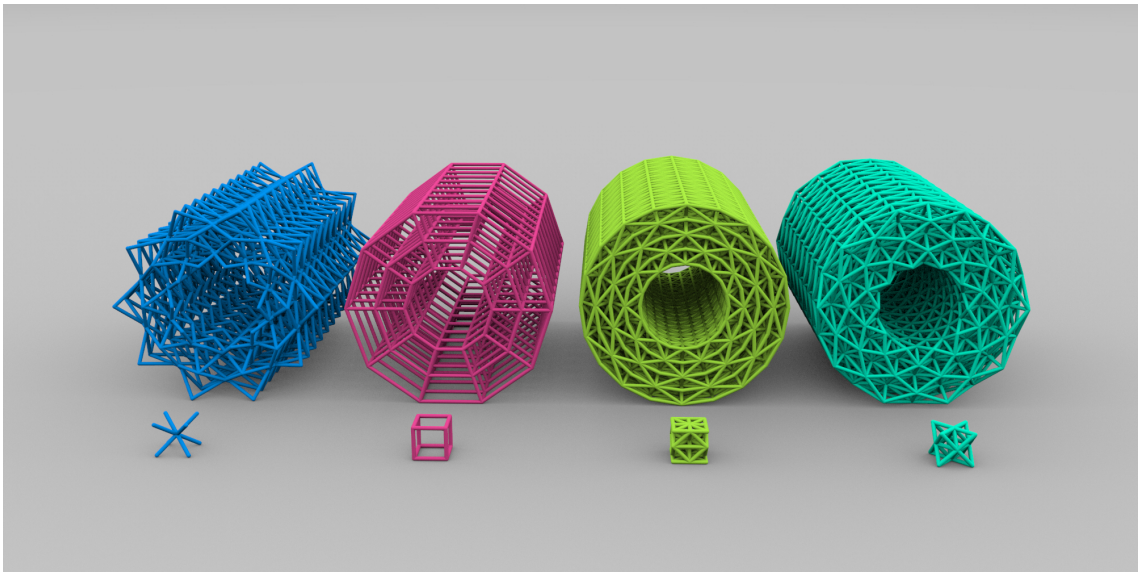

Figure 18: Lattice RVEs used for example 2. Source: own (LNG).

Figure 18 illustrates similar geometries we have tested. In front of each one,there are the RVE patterns configuring the lattice structure behind. Denoting them from left to right, we used the X-shape (dark blue), the cube (pink), the six-tetrahedral-cube (green) and the octet-truss (turquoise). These cylinders have fifteen layers in the azimuth direction, fifteen repetitions in the longitudinal-axis direction (cylinder's length) and two layers in radial-axis direction. Therefore, $(n_X, n_Y, n_Z) = (15, 15, 2)$ are the RVE quantity in each axis of repetition of the lattices. In the test samples we also used have used $(n_X, n_Y, n_Z) = (15, 15, 1)$.

We define the cell size dimensions to be $2.0\,\text{mm} \times 2.0\,\text{mm} \times 2.0\,\text{mm}$. We define the inner beams to have square cross-section with side length a. The values of a are chosen so that the volume of the lattice itself for each cylinder keeps constant as in the previous example. Table 3 displays the relevant information about the material data and the dimensions of the structure.

Finally, we work with Openseespy to compile the FEA. Concluding the simulation for each of the lattice patterns, we post-process the results using COMSOL. Figure 19 shows the resulting stress state of two of the tested cases after applying gravity load. Please note that Appendix A, figure A1, includes the stress plots of the four cases but the ones shown is this section are the most illustrative.

Table 3: Cylinder tests data.

Material data		
Young's modulus		2×10^9 Pa
Poisson's ratio		0.25
Density		1040 Kg m^{-3}
Dimensions		
Cell-size, cube side length		2.0 mm
Cylinder's global length		30.0 mm
Cylinder's global inner radius		3.0 mm
Volume lattice structure		1.075×10^2 mm^2
Cross-section data, a		
Case	Pattern	Side length, a m
1	Cube	2.516×10^{-1} mm
2	X-shape	2.095×10^{-1} mm
3	Six-tetrahedral-cube	1.000×10^{-1} mm
4	Octet-truss	1.230×10^{-1} mm

From figure 19 we can appreciate that the RVEs configuration affects indeed on the lattice structure behaviour. At first sight, one can appreciate that the appearance of Von Misses stresses field through the global cylinder domain is distributed following different schemes for case 1 than for case 4. Furthermore, case 1 presents local effects in the nodal zones of the lattice while case 4 is almost not having them. A third contrast we observe is that the sign of the curvature of the overall cylinder through the X axis in case 1 is nearly being the opposite than for case 4.

Finally, table 4 shows the mean deflection of the nodes of the structures at the free edge. We can see that each case presents different mean nodal displacement. Note that case 3 and 4 are being apparently stiffer than case 1 and 2 in bending due to the fact that the displacements are smaller.

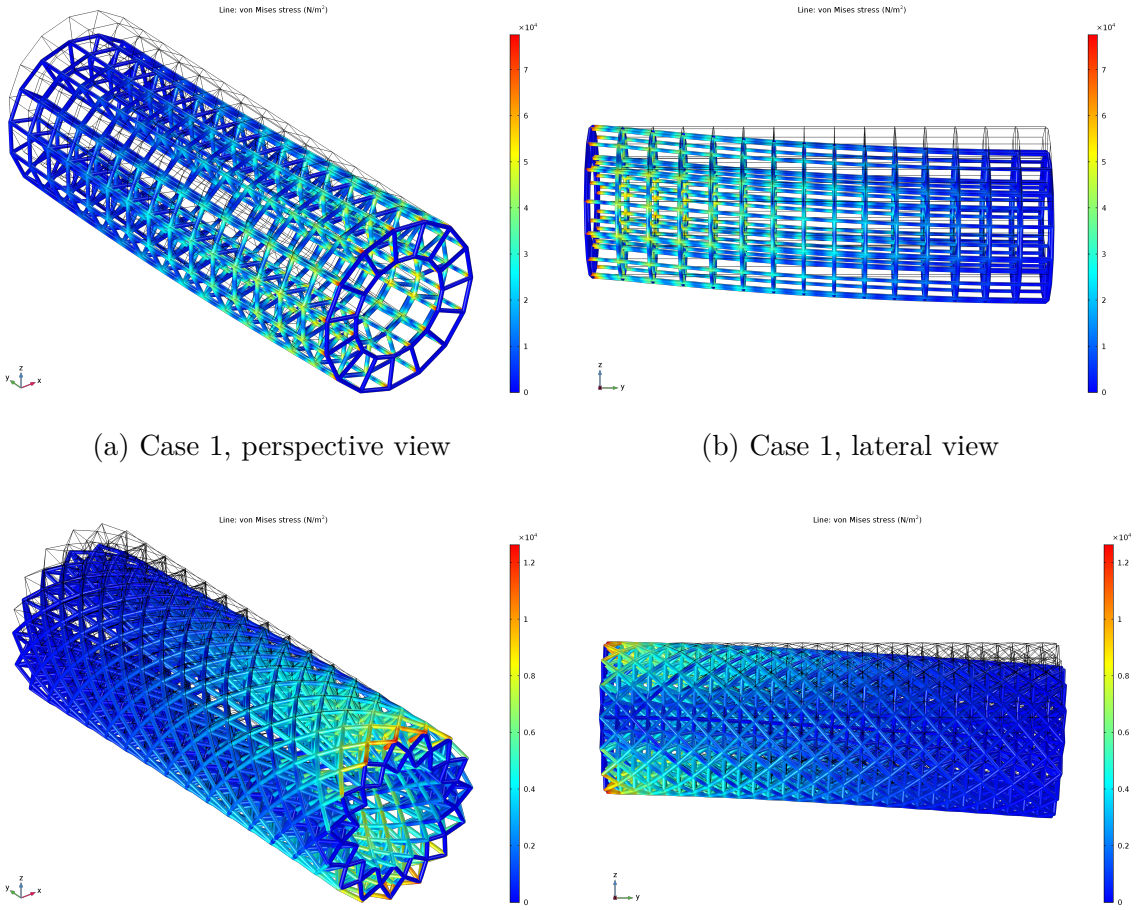

(a) Case 1, perspective view

(b) Case 1, lateral view

(c) Case 4, perspective view

(d) Case 4, lateral view

Figure 19: Resulting Von Misses stress state of two different lattice cylinders. Subfigure a) and b) correspond to the cubic pattern and figure c) and d) correspond to the octet-truss pattern.

Table 4: Mean nodal displacement at the free edge.

Case	Pattern	Displacement (-Z axis)
1	Cube	1.295×10^{-3} mm
2	X-shape	5.027×10^{-3} mm
3	Six-tetrahedral-cube	2.739×10^{-4} mm
4	Octet-truss	4.924×10^{-4} mm

4.3 Modelling imperfections in lattice structures

In this example we want to study the effect of imperfections in the lattice beams which can be in wrong state and do not carry the stress they are supposed to. Such imperfections may exist in real structures due to manufacturing errors or some other reasons. Thus, we delete some struts member of RVEs to not consider their contribution to the structure strength.

In this example, we test lattice octet-truss cylinders, from section 4.2, case 4. The objective now is to estimate the relative difference we get on the displacement, at the free edge, of an abnormal cantilever cylinder compared with a perfect one. The abnormal lattice cylinder has a fixed percentage of beams missing. The scope is to integrate LNG in a practical application of the manufacturing stage. We use Monte Carlo method to carry out.

Monte Carlo method is a subset of computational algorithms that utilize the process of repeated random sampling to make numerical estimations of unknown parameters, also called "quantity of interest" [67]. In this example, the quantity of interest is the relative difference of displacement and the random samples are the different set of deleted edges of the cylinder.

The general steps of a Monte Carlo simulation are the following [68]:

- **Step 1**: Define a domain of possible inputs.
- **Step 2**: Generate random samples following a probability distribution over the domain. This will generate a set of inputs.
- **Step 3**: Perform a deterministic computation on the inputs.
- **Setp 4**: Aggregate the resulting "quantity of interest" and perform a statistical analysis of it.

Following these four steps, we start with defining the edges as the domain of possible input. We fix a percentage of wrong state beams over the total number which is the mean of the probability distribution. Then, following a uniform probability distribution, each edge has the same probability to be deleted, we generate a set of samples. Then, we perform the deterministic computation that in this case starts deleting the edges of them from the original (perfect) model. Next, we compute the FEA under an edge load, F. Finally, we keep the quantity of interest, i.e. the displacement at the free edge and we calculate the relative difference from the displacement we got for the perfect case. This process, is carried out in an iterative loop covering each sample. Consecutively, we get the following frequency distributions for each percentage. See figures 20, 21 and 22.

Looking at the figures, we can see how the relative difference is increasing with the percentage of deleted beams of the lattice. The most frequent value of the

displacement relative difference and the standard deviation are gradually increasing with the deleted beams percentage. This finding is totally reasonable with the test due to the fact that the more beams the cylinder is missing, the less capability it has to bear the load.

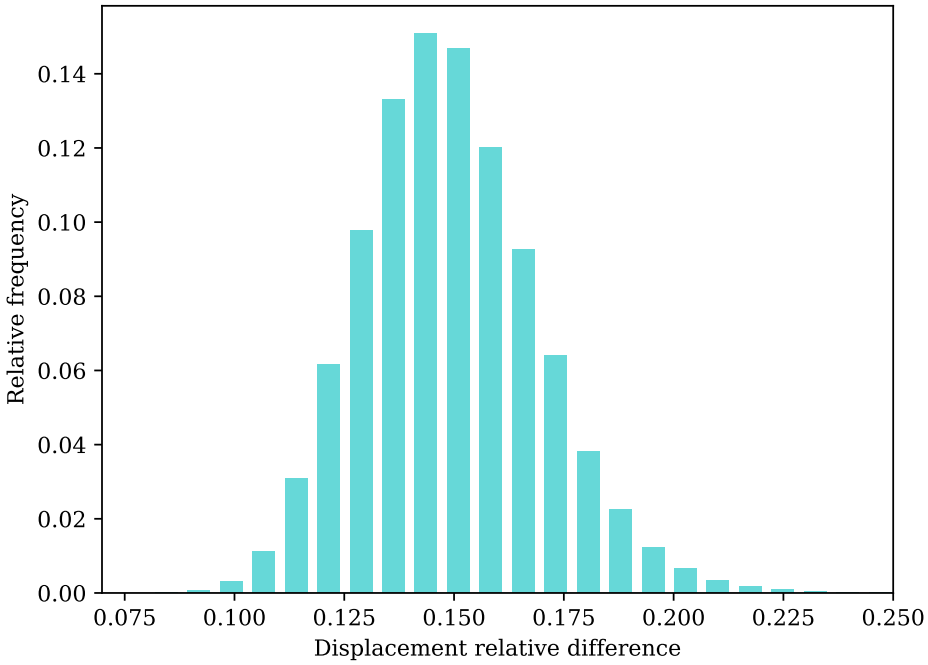

Figure 20: Percentage of deleted beams = 5% (50000 samples).

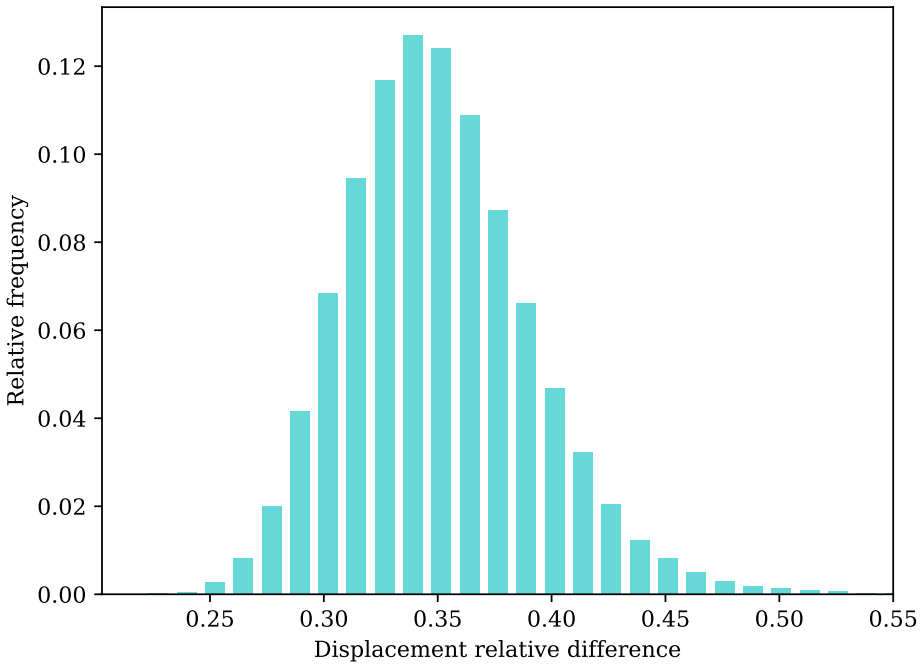

Figure 21: Percentage of deleted beams = 10% (50000 samples).

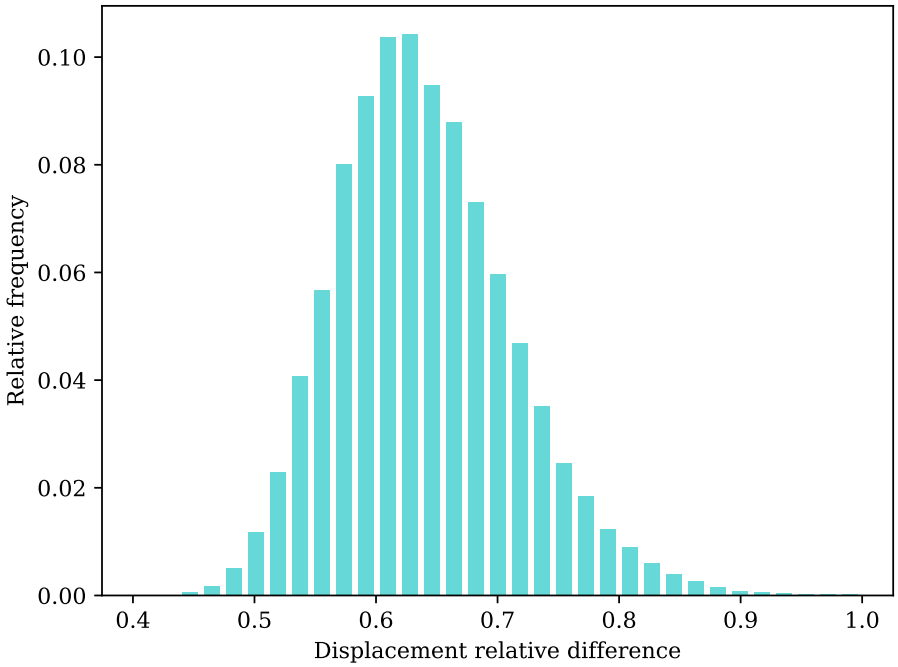

Figure 22: Percentage of deleted beams = 15% (50000 samples).

4.4 Using strain gradient theory for homogenization of lattice structures

This example focuses on applying the strain gradient elasticity theory for modeling the size-dependent mechanical response of a lattice beam in bending. The goal is to show the usefulness of including the LNG in a routine to study homogenized lattice structures' properties. In addition, due to the technical details of this example, we attempt to give first an outline of the theory applied.

4.4.1 Theoretical background

It is well known that important decisions in modeling engineering problems include the reduction of the physical problem into a general mathematical problem and, further, the simplification of the mathematical problem itself [69]. In case of lattice structures, these steps are deeply being studied in order to minimize the error induced in between. In prior, it seems they can be analyzed as classical frame structures and, therefore, these steps would not differ from what has already been solved before. However, they can have complex geometrical configurations with also large amount of elements defining them that result in time and space computational problems when carrying out the numerical analysis. Hence, it is fundamental to come up with an approach able to reduce the model complexity but minimizing the simplification error.

The first idea in this modeling decision process is to treat lattice structures accounting only the global shape they have, i.e. the lattice geometry is reduced to homogeneous geometry. For this reason, next step is to find a replacement homogeneous material with properties equivalent to those of the original structure. Hence, the objective is to study the lattice configuration in order to find the effective properties of the equivalent homogenized material. The mathematical theory of homogenization have been developed since it first showed up in the 1970's [70, 71].

For structural analysis, classical continuum elasticity theory has prevailing for modelling and analysis structures in science and engineering [65]. However, a fundamental notion of this theory is that the length scale over which deformation varies is much larger than the discrete length of the matter, [71]. Consequently, this theory is not able to capture size effects of lattice structures related with the inner micro-structure and the global size - i.e. it does not account the relation of the lattice cell or RVE with the global structure.

Alternatively, strain gradient elasticity theory is proposed [73]. This one include terms in the energy formulations that account for the micro-structure configuration and consequently adding length scale material parameters to the equations. Moreover, multiple generalizations on strain gradient elasticity theory have been derived for dimensional reduced structural models [65, 72].

The examples we present are related with the validation of the strain gradient

elasticity model formulation. In particular, we focus on the generalized strain gradient elasticity for Euler-Bernoulli beam model. Hence, we consider the static Euler-Bernoulli beam problem, fixed at $X = 0$ and with a bending transverse load, F at the free edge, $X = L$ as proposed in [64, 72]. Reference[64] consider the derived generalized equations derived in [69, 72]. Reference [64] presents the normalized bending rigidity equation (1) for rectangular cross-sections in the following form:

$$\frac{D}{D_0} = 1 + 12\frac{g^2}{h^2} \tag{1}$$

- D_0 is the bending rigidity within classical Euler-Bernoulli model,

$$D = F/w^{FE} \tag{2}$$

- D is the bending rigidity gotten from the numerical analysis,

$$D_0 = F/w_{cl}^{BE} \tag{3}$$

where w_{cl}^{BE} is the deflection at point $X = L$, g the structural length scale parameter and h the height of the beam. In this example, we study the size-dependant mechanical response of lattice beams in bending. The general idea is to analyze beams subjected to the same mechanical conditions but having different inner lattice configurations. The goal is to include LNG in a scripted routine which allow us to test any desired geometry in a simple and fast manner.

The mechanical conditions we use in these lattice beam models are the following:

1. The beam is clamped at the left hand side, $X = 0$.
2. The beam has a free edge at the right hand side, $X = L$ where L is the length of the global beam structure.
3. The beam has a point load at the right hand side, $X = L$, that translates into a multi-point load at the lattice nodes belonging to $X = L$ boundary.

Regarding the model dimensions of the examples we show, we apply two approaches, a 2D model and a 3D model. Therefore, the 2D model is a 2D lattice structure beam whose inner lattice beams are numerically threaded as 2D Euler-Bernoulli beam elements and the 3D model is indeed a 3D lattice structure beam whose inner lattice beams are 3D Euler-Bernoulli beam elements.

4.4.2 2D lattice

In the 2D model we tried to replicate the same experiment presented in [64]. The geometry of the lattice structure is configured with a triangular RVE with dimensions as showed in figure 23. The study consist on creating multiple lattice structure configurations with different inner densities but always conserving the ratio between

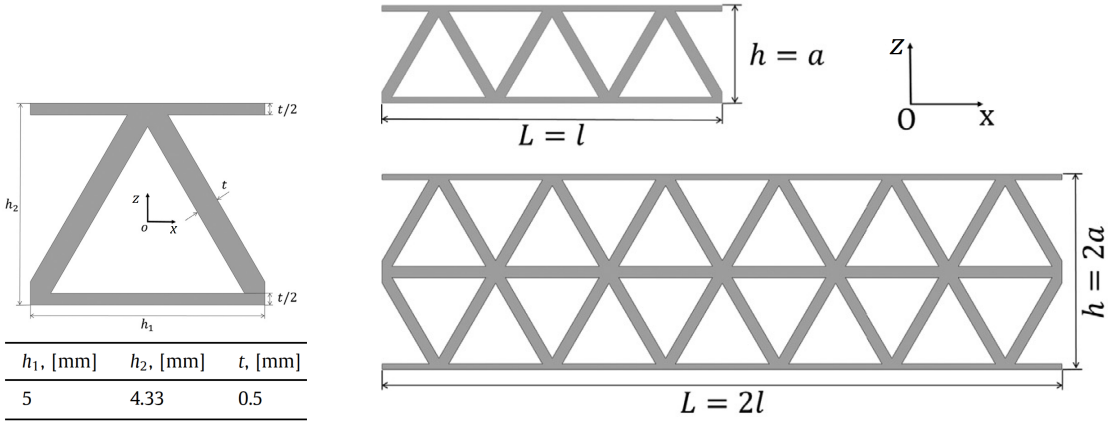

h_1, [mm]	h_2, [mm]	t, [mm]
5	4.33	0.5

(a) RVE dimensions.

(b) Lattice proportions.

Figure 23: Lattice structure parameters. Source: [64].

length and height, and also maintaining the cell-size of the RVE. In this particular case, we apply a ratio length-height of 20.785 that means the ratio between X-axis and Z-axis RVE densities is 18. Note that we replicate the RVE by applying mirroring in each direction.

Next step consist on simulating each sample model with FEM. From the FEA solution we keep the nodal displacements at the free-edge and then we calculate the mean. After carrying out the pertinent simulations and post-processing the results, we can obtain the normalized bending rigidity values for each of the studied beams. The normalized bending rigidity is calculated as in equation (2) and (3).

For the 2D triangular beam, we have obtained the points (red points and black crosses) of the graphs shown in figures 24a and 24b, respectively. Figure 24a shows the data points from the simulations in red and then the curve representing equation (1) (green dotted curve and black dotted curve). The green curve has been obtained fitting g and E to the equation, however, this is not the usual manner to obtain them. For this reason, we have also plot figure 24b which uses E obtained from homogenizing the triangular RVE and then, we have fitted g to the data points. In this figure, we show colored curves obtained using similar g values to the one we fit. On the right, the color-bar shows the range of g values. Additionally, in both plots we have drawn the grey dashed line according to the Classical Elasticity Theory, i.e. $g = 0$.

Looking at figure 24, one can recognize the size effects of the 2D beam by simply looking a the points representing the FEA result with the different lattice structure configurations. We see how the total height of the structure is affecting the relative rigidity. Remember that the total height of the structure is directly related with the number of lattice inside the structure due to the fact that the RVEs size is conserved for all the specimens that are analyzed. Consequently, due to the nature of the

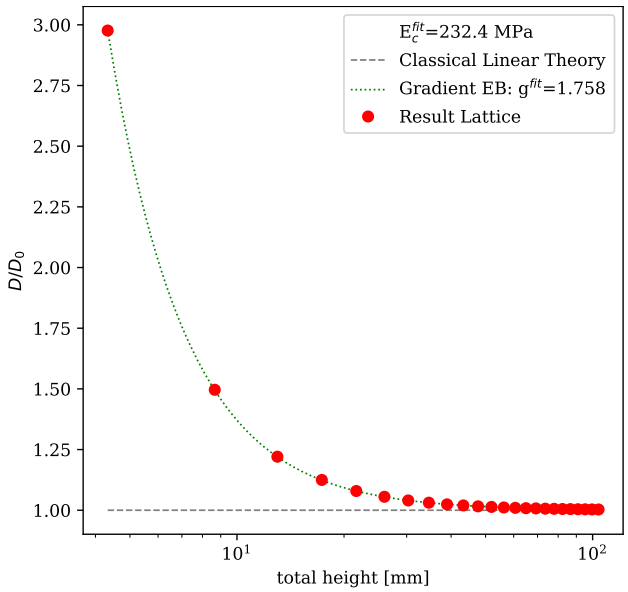

(a)

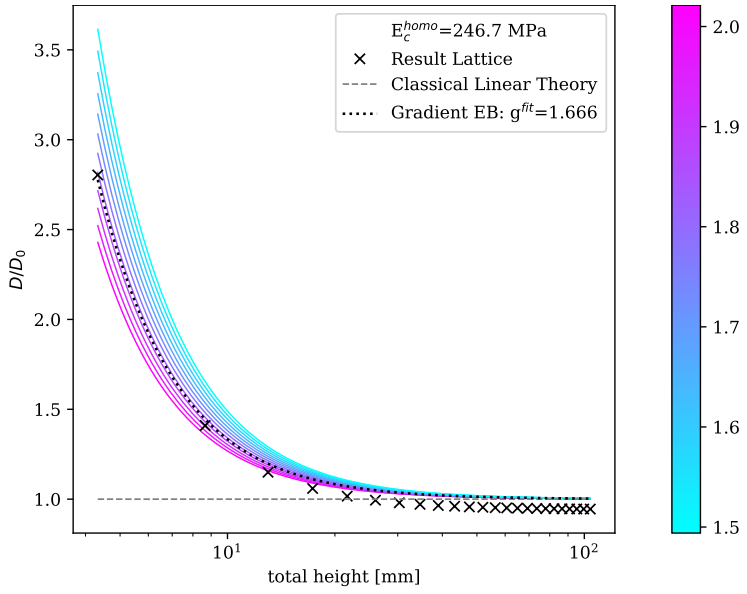

(b)

Figure 24: Normalized bending rigidity for a lattice 2D beam with overall length/height = 20.785. Source: own.

inner lattice configuration as the micro-structure, the homogeneity of the global beam is lower for small RVEs density inside the structure than for larger amounts. Accordingly, the beam is becoming more homogeneous as the RVEs density increase, until reaching a certain stability when one can not observe differences on the global beam performance regarding its rigidity.

On the other hand, it is relevant to note the difference on the curves we show on figures 24a and 24b is indeed because they are obtained using different g and E. As we mentioned, the common procedure starts by doing the homogenization test and obtain the effective E and then fit g based on the test data. This usually give a good curve fitting but in this example we have obtained a curve that is quite far from the points. Checking (2) and observing the good fitting we obtain in figure 24a we conclude that the E is not completely corresponding to the test data. Hence, assuming that E from the homogenization test is right, we deduce that the fact that we have used Euler-Bernoulli beam elements for the lattice beams results in an underestimation of the structure stiffness. This can be seen looking on the fitted E which is lower than the one from homogenization test.

As an extra work we add figure 25 aiming to show the sensitivity of the inner height modeled and the length-scale parameter g. The three colored curves represent, again, the rigidity of the Euler-Bernoulli beam for the generalized gradient elasticity, equation (2). The overall structure is having same dimensions as the ones described before, in the first example, but the distinction between the curves is that the structures modeled diverge in the inner RVE's beam heights. We can observe that the specimen with larger beam height (h=2.000 mm, yellow curve) is lightly close to the classical curve (dashed grey straight line) compared to the two others. Therefore, the fitted g parameter is also resulting in lower values due to the fact that it is related to the curvature of the previously referred equation. The opposite happens with the smaller height (h=2.000 mm, dark blue curve). Additionally, note that the resulting effective Young modulus (fitted with the data points) increase as well with the height, having a larger effective density, thus, building a stiffer global structure.

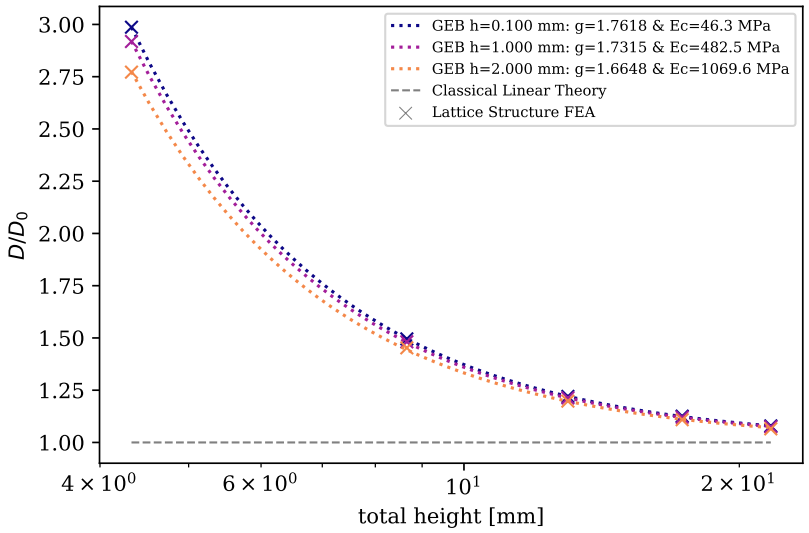

Figure 25: Normalized bending rigidity for the lattice 2D beam with length/height = 20.785 for different inner lattice beam heights (different colours) and increasing overall height (X-axis).

4.4.3 3D lattice

In the 3D model we use the octet-truss as RVE showed in previous examples. We keep constant RVE density in the new dimension (Y-axis) representing the width of the beams. Analogously, we create multiple lattice structure configurations. The ratios length-height on these simulations are 5.0 and 8.0 (ratio between RVEs in X-axis and Z-axis), because in this case, the cell-size is equal in all directions.

Figure 26 and 27 show the results obtained with 3D structures analogously to the 2D lattice. In this case, besides showing the effect of the size effects and evaluating the fitting of (1), we want to capture the effects of increasing the RVE in Y-axis as well. Thereupon, we tested specimens with various RVE densities inside in the following manner. For example, figures [26a, 26b, 27a, 27b], represent specimens with ratio of longitudinal to height dimensions of RVE equal to 5 and width equal to 1 RVE and 2 RVE, respectively. Then, figures [26c - 26f, 27c - 27f], have a ratio length-height of 8. Analyzing them, first we observe that the curve is not well fitted in some of the specimen, specially for those ones that has less RVEs in width.

We found differences, as previous case, with the curves of figures 26 and 27 due to the difference on the procedure for obtaining g and E. Young modulus used for 27 is obtained from equation 4 in [57] approaching an equivalent value which would be obtained by homogenization. Finally, we can conclude that for 3D beams the modelling methods we have used are not ideal and should be improved.

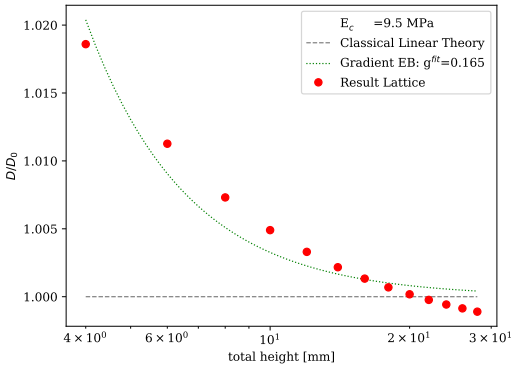

(a) length/height = 5, width = 1 RVE

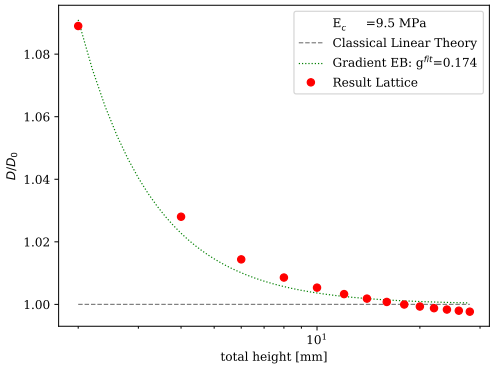

(b) length/height = 5, width = 2 RVE

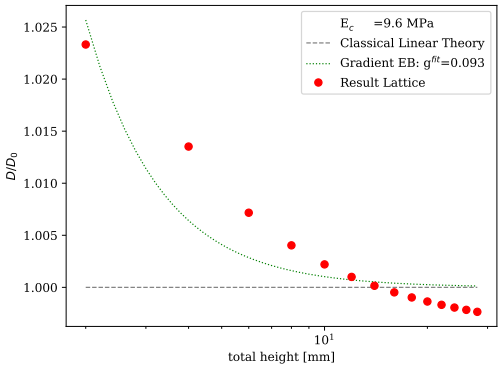

(c) length/height = 8, width = 2 RVE

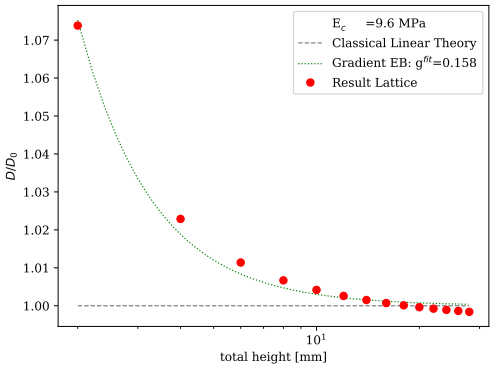

(d) length/height = 8, width = 3 RVE

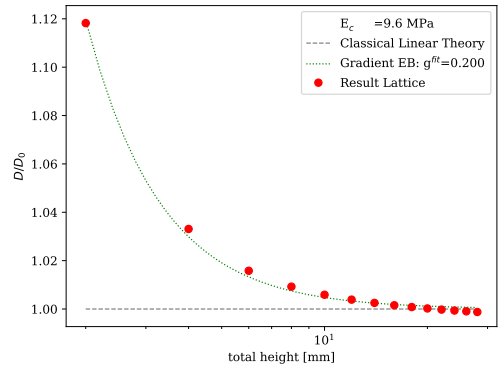

(e) length/height = 8, width = 4 RVE

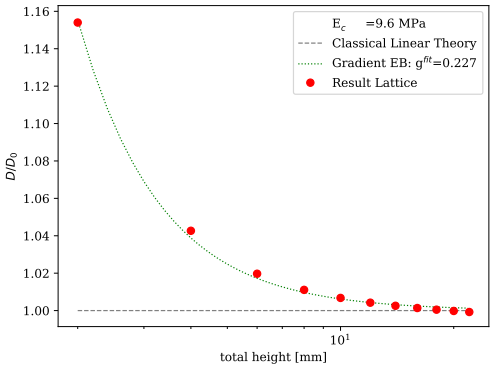

(f) length/height = 8, width = 5 RVE

Figure 26: Normalized bending rigidity for 3D beam with octet-truss with fitting on g and E parameters.

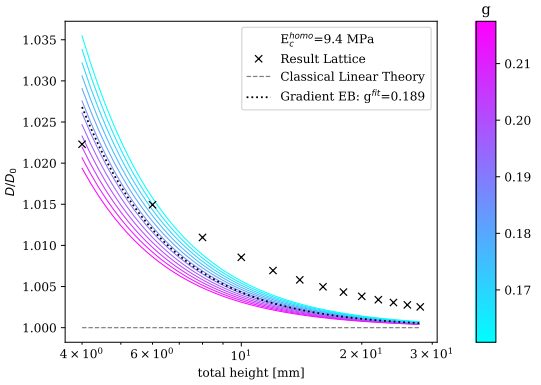

(a) length/height = 5, width = 1 RVE

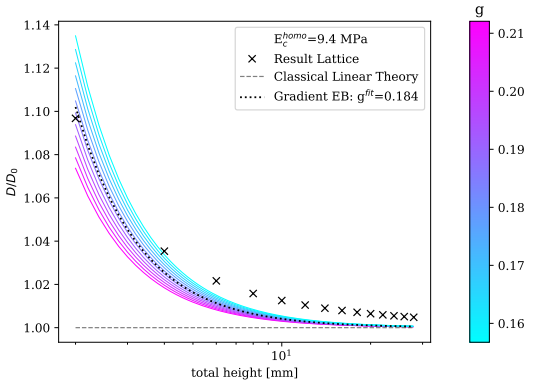

(b) length/height = 5, width = 2 RVE

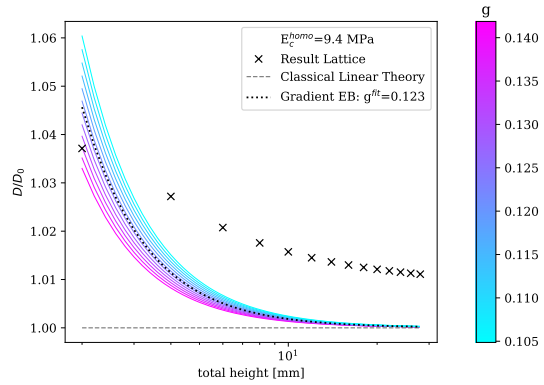

(c) length/height = 8, width = 2 RVE

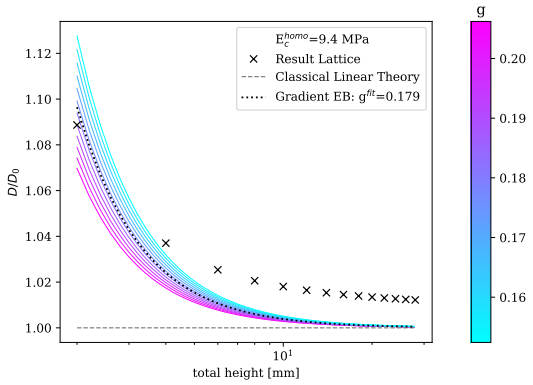

(d) length/height = 8, width = 3 RVE

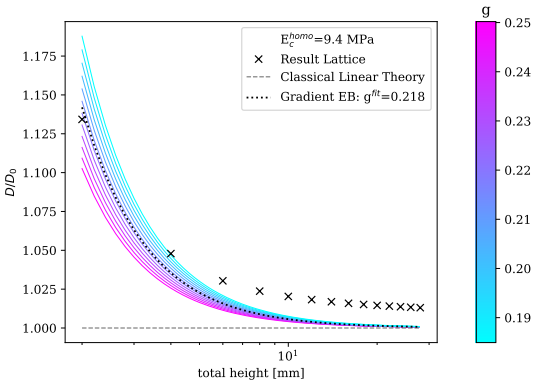

(e) length/height = 8, width = 4 RVE

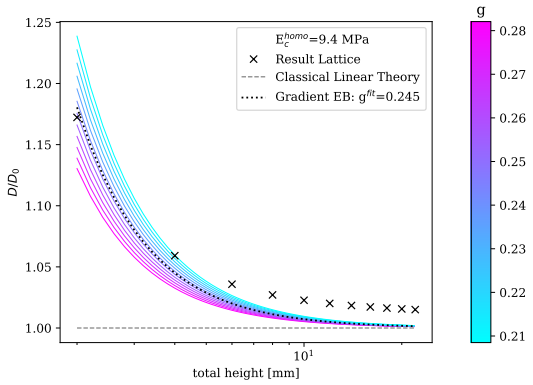

(f) length/height = 8, width = 5 RVE

Figure 27: Normalized bending rigidity for 3D beam with octet-truss with E from homogenization test and a fitted g.

4.5 The octet-truss plate

We finalize the examples section simulating an octet-truss lattice plate. We model several plates with different inner quantities of RVE in each direction. We consider a cantilever plate in the same conditions of example 1. Then, we execute the FEA and we show the results. In the same line as the previous example, we aim to capt size-effects on the plate due to the lattice configurations.

We define the quadrangular lattice plate which has a RVEs ratio height to length of 5. Then, we create a few geometries continuously increasing the height of the lattice plate i.e. the side length by adding more lattice RVEs. The beams configuring the lattice have a height of 0.1 mm and the RVE cell size is $2.0\,\text{mm} \times 2.0\,\text{mm} \times 2.0\,\text{mm}$. The material parameters are the same we have been utilized in all the examples, shown in table 1.

After carrying out the FEA we obtain figure 28. The y-axis of the plot is showing the displacement of the free-edge of the plate ($X = L$). In order to make the displacement dimensionless, we have divided the resulting values by the maximum value we get (that in this case is obtained for the smaller height plate).

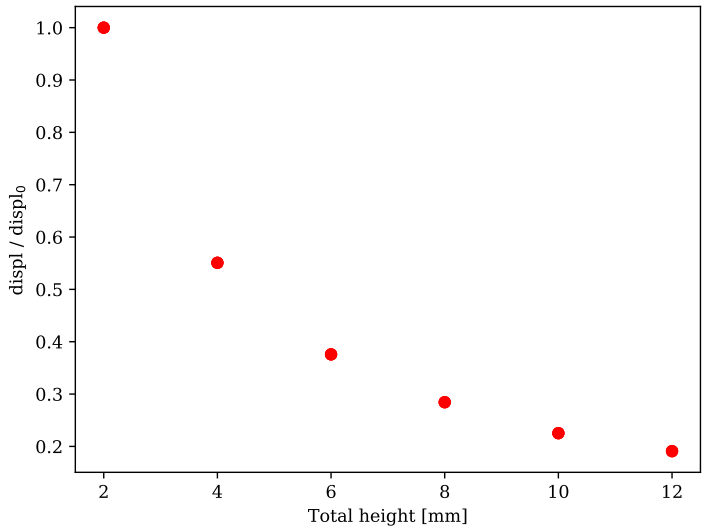

Figure 28: Results of the lattice octet-truss plate.

From this figure, we see that the displacements decrease as the height of the plate increases. Moreover, we observe that the trend of the results has a shape similar to the previous example not being constant neither lineal. Hence, we can conclude that we observe size effects on the plate.

5 Discussion and conclusions

In this work we have studied lattice structures and analyzed the current available software for simulation and research. As a result, the work concludes with a scripted tool, named LNG, written and collect it as a Python Package. It is created with the idea of contributing to the scientific field, bringing an open-source option for generation of lattice structures geometry so as to study their impressive properties.

We have gone inside geometrical problems to provide a tool that has been coded with a lot of effort to be efficient, computationally talking. It is produced with the idea of granting a customizable engine able to reproduce multiple lattice structures. LNG provides easy integrability of FEA and simple implementation of iterative analysis.

An important part of the work is devoted to testing LNG in different examples. We have focused on the analysis of elastic properties of lattices. Through the examples, we have explored different particular characteristics of lattice structures. First, we have shown the wide range of behaviours lattices can have by changing the RVEs of their grid. Moreover, we have seen the sensitivity of the inner elements and contribution to the overall lattice performance. Finally, we have shown the size effects they have when varying the inner density and configuration of their net.

As a conclusion, we could say that LNG is a useful tool and facilitates lattice structures study. We have proposed further improvements for LNG which can be implemented as future works.

References

[1] Wadley, H.N.G., 2002. Cellular Metals Manufacturing. Advanced Engineering Materials 4, 726–733.https://doi.org/10.1002/1527-2648(20021014)4:10<726::aid-adem726>3.0.co;2-y

[2] Bull. Amer. Math. Soc. 70 (1964), no. 4, 468–481.https://projecteuclid.org/euclid.bams/1183526078

[3] Abueidda, D.W., Jasiuk, I., Sobh, N.A., 2018. Acoustic band gaps and elastic stiffness of PMMA cellular solids based on triply periodic minimal surfaces. Materials & Design 145, 20–27.https://doi.org/10.1016/j.matdes.2018.02.032

[4] Ashby, M., 2013. Designing architectured materials. Scripta Materialia 68, 4–7.https://doi.org/10.1016/j.scriptamat.2012.04.033

[5] Ashby, M.., 2005. The properties of foams and lattices. Philosophical Transactions of the Royal Society A: Mathematical, Physical and Engineering Sciences 364, 15–30.https://doi.org/10.1098/rsta.2005.1678

[6] Austermann, J., Redmann, A.J., Dahmen, V., Quintanilla, A.L., Mecham, S.J., Osswald, T.A., 2019. Fiber-Reinforced Composite Sandwich Structures by Co-Curing with Additive Manufactured Epoxy Lattices. Journal of Composites Science 3, 53.https://doi.org/10.3390/jcs3020053

[7] Azman, A.H., 2017. Method for integration of lattice structures in design for additive manufacturing.

[8] Azman, A.H., Vignat, F., Villeneuve, F., 2015. Design Configurations and Creation of Lattice Structures for Metallic Additive Manufacturing.

[9] Banhart, J., 2001. Manufacture, characterisation and application of cellular metals and metal foams. Progress in Materials Science 46, 559–632.https://doi.org/10.1016/s0079-6425(00)00002-5

[10] Bauer, J., Schroer, A., Schwaiger, R., Kraft, O., 2016. Approaching theoretical strength in glassy carbon nanolattices. Nature Materials 15, 438–443.https://doi.org/10.1038/nmat4561

[11] Brackett, D.J., Ashcroft, I.A., Wildman, R.D., Hague, R.J.M., 2014. An error diffusion based method to generate functionally graded cellular structures. Computers Structures 138, 102–111.https://doi.org/10.1016/j.compstruc.2014.03.004

[12] Brennan-Craddock, J., Brackett, D., Wildman, R., Hague, R., 2012. The design of impact absorbing structures for additive manufacture. Journal of Physics: Conference Series 382, 12042.https://doi.org/10.1088/1742-6596/382/1/012042

[13] Dantas, A.C.S., Scalabrin, D.H., De Farias, R., Barbosa, A.A., Ferraz, A.V., Wirth, C., 2016. Design of Highly Porous Hydroxyapatite Scaffolds by Conversion of 3D Printed Gypsum Structures – A Comparison Study. Procedia CIRP 49, 55–60.https://doi.org/10.1016/j.procir.2015.07.030

[14] Del Olmo, E., Grande, E., Samartin, C.R., Bezdenejnykh, M., Torres, J., Blanco, N., Frovel, M., Cañas, J., 2012. Lattice structures for aerospace applications. European Space Agency, (Special Publication) ESA SP. 691.

[15] Dong, G., Tang, Y., Zhao, Y.F., 2017. A Survey of Modeling of Lattice Structures Fabricated by Additive Manufacturing. Journal of Mechanical Design 139, 100906.https://doi.org/10.1115/1.4037305

[16] Dumas, M., Terriault, P., Brailovski, V., 2017. Modelling and characterization of a porosity graded lattice structure for additively manufactured biomaterials. Materials Design 121, 383–392.https://doi.org/10.1016/j.matdes.2017.02.021

[17] Egan, P.F., Gonella, V.C., Engensperger, M., Ferguson, S.J., Shea, K., 2017. Computationally designed lattices with tuned properties for tissue engineering using 3D printing. PLOS ONE 12, e0182902.https://doi.org/10.1371/journal.pone.0182902

[18] Evans, A., 1998. Multifunctionality of cellular metal systems. Progress in Materials Science 43, 171–221.https://doi.org/10.1016/s0079-6425(98)00004-8

[19] Evans, A.G., Hutchinson, J.W., Fleck, N.A., Ashby, M.F., Wadley, H.N.G., 2001. The topological design of multifunctional cellular metals. Progress in Materials Science 46, 309–327.https://doi.org/10.1016/s0079-6425(00)00016-5

[20] Fleck, N., 2004. An overview of the mechanical properties of foams and periodic lattice materials. Cell Met Polym.

[21] Fleck, N.A., Deshpande, V.S., Ashby, M.F., 2010. Micro-architectured materials: past, present and future. Proceedings of the Royal Society A: Mathematical, Physical and Engineering Sciences 466, 2495–2516.https://doi.org/10.1098/rspa.2010.0215

[22] Front Matter, 2018. , in: Design and Analysis of Tall and Complex Structures. Elsevier, pp. i–ii.https://doi.org/10.1016/b978-0-08-101018-1.09988-3

[23] Gibson, L., Ashby, M., 1999. Cellular Solids: Structure and Properties, Cambridge University Press: Cambridge, UK, .

[24] Gilbert, M., Tyas, A., 2003. Layout optimization of large-scale pin-jointed frames. Engineering Computations 20, 1044–1064.https://doi.org/10.1108/02644400310503017

[25] Helou, M., Kara, S., 2017. Design, analysis and manufacturing of lattice structures: an overview. International Journal of Computer Integrated Manufacturing 31, 243–261.https://doi.org/10.1080/0951192x.2017.1407456

[26] Ingrid P., Lorenzo C., 2018. The Evolution of 3D Printing in AEC: From Experimental to Consolidated Techniques, 3D Printing, Dragan Cvetković, IntechOpen, DOI: 10.5772/intechopen.79668. Available from: https://www.intechopen.com/books/3d-printing/the-evolution-of-3d-printing-in-aec-from-experimental-to-consolidated-techni

[27] Kirsch, K.L., Thole, K.A., 2017. Pressure loss and heat transfer performance for additively and conventionally manufactured pin fin arrays. International Journal of Heat and Mass Transfer 108, 2502–2513.https://doi.org/10.1016/j.ijheatmasstransfer.2017.01.095

[28] Laskar, R., 1967. A characterization of cubic lattice graphs. Journal of Combinatorial Theory 3, 386–401.https://doi.org/10.1016/s0021-9800(67)80105-4

[29] Maskery, I., Aboulkhair, N.T., Aremu, A.O., Tuck, C.J., Ashcroft, I.A., 2017. Compressive failure modes and energy absorption in additively manufactured double gyroid lattices. Additive Manufacturing 16, 24–29.https://doi.org/10.1016/j.addma.2017.04.003

[30] Maskery, I., Hussey, A., Panesar, A., Aremu, A., Tuck, C., Ashcroft, I., Hague, R., 2016. An investigation into reinforced and functionally graded lattice structures. Journal of Cellular Plastics 53, 151–165.https://doi.org/10.1177/0021955x16639035

[31] Matlack, K.H., Bauhofer, A., Krödel, S., Palermo, A., Daraio, C., 2016. Composite 3D-printed metastructures for low-frequency and broadband vibration absorption. Proceedings of the National Academy of Sciences 113, 8386–8390.https://doi.org/10.1073/pnas.1600171113

[32] Mines, R.A.W., Tsopanos, S., Shen, Y., Hasan, R., McKown, S.T., 2013. Drop weight impact behaviour of sandwich panels with metallic micro lattice cores. International Journal of Impact Engineering 60, 120–132.https://doi.org/10.1016/j.ijimpeng.2013.04.007

[33] Ozdemir, Z., Tyas, A., Goodall, R., Askes, H., 2017. Energy absorption in lattice structures in dynamics: Nonlinear FE simulations. International Journal of Impact Engineering 102, 1–15.https://doi.org/10.1016/j.ijimpeng.2016.11.016

[34] Panesar, A., Abdi, M., Hickman, D., Ashcroft, I., 2018. Strategies for functionally graded lattice structures derived using topology optimisation for Additive Manufacturing. Additive Manufacturing 19, 81–94.https://doi.org/10.1016/j.addma.2017.11.008

[35] Panesar, A., Ashcroft, I., Brackett, D., Wildman, R., Hague, R., 2017. Design framework for multifunctional additive manufacturing: Coupled optimization strategy for structures with embedded functional systems. Additive Manufacturing 16, 98–106.https://doi.org/10.1016/j.addma.2017.05.009

[36] Paoletti, I., Ceccon, L., 2018. The Evolution of 3D Printing in AEC: From Experimental to Consolidated Techniques, in: 3D Printing. InTech.https://doi.org/10.5772/intechopen.79668

[37] Rashed, M.G., Ashraf, M., Mines, R.A.W., Hazell, P.J., 2016. Metallic microlattice materials: A current state of the art on manufacturing, mechanical properties and applications. Materials Design 95, 518–533.https://doi.org/10.1016/j.matdes.2016.01.146

[38] Refai, K., Montemurro, M., Brugger, C., Saintier, N., 2019. Determination of the effective elastic properties of titanium lattice structures. Mechanics of Advanced Materials and Structures 1–14.https://doi.org/10.1080/15376494.2018.1536816

[39] RYAN, G., PANDIT, A., APATSIDIS, D., 2006. Fabrication methods of porous metals for use in orthopaedic applications. Biomaterials 27, 2651–2670.https://doi.org/10.1016/j.biomaterials.2005.12.002

[40] Smith, C.J., Gilbert, M., Todd, I., Derguti, F., 2016. Application of layout optimization to the design of additively manufactured metallic components. Structural and Multidisciplinary Optimization 54, 1297–1313.https://doi.org/10.1007/s00158-016-1426-1

[41] Suard, M. Characterization and optimization of lattice structures made by Electron Beam Melting. (2015)

[42] Sung, C.H., Lee, K.S., Lee, K.S., Oh, S.M., Kim, J.H., Kim, M.S., Jeong, H.M., 2007. Sound damping of a polyurethane foam nanocomposite. Macromolecular Research 15, 443–448.https://doi.org/10.1007/bf03218812

[43] Suralvo, M., Bouwhuis, B., McCrea, J.L., Palumbo, G., Hibbard, G.D., 2008. Hybrid nanocrystalline periodic cellular materials. Scripta Materialia 58, 247–250.https://doi.org/10.1016/j.scriptamat.2007.10.018

[44] Tang, Y., Dong, G., Zhou, Q., Zhao, Y.F., 2018. Lattice Structure Design and Optimization With Additive Manufacturing Constraints. IEEE Transactions on Automation Science and Engineering 15, 1546–1562.https://doi.org/10.1109/tase.2017.2685643

[45] Tang, Y., Zhao, Y.F., 2016. A survey of the design methods for additive manufacturing to improve functional performance. Rapid Prototyping Journal 22, 569–590.https://doi.org/10.1108/rpj-01-2015-0011

[46] Thai, H.-T., Choi, D.-H., 2013. Size-dependent functionally graded Kirchhoff and Mindlin plate models based on a modified couple stress theory. Composite Structures 95, 142–153.https://doi.org/10.1016/j.compstruct.2012.08.023

[47] Tóth, L. F. What the bees know and what they do not know. What the bees know and what they do not know. Bull. Amer. Math. Soc. 70 (1964), no. 4, 468–481. https://projecteuclid.org/euclid.bams/1183526078

[48] Wadley, H.N.., 2005. Multifunctional periodic cellular metals. Philosophical Transactions of the Royal Society A: Mathematical, Physical and Engineering Sciences 364, 31–68.https://doi.org/10.1098/rsta.2005.1697

[49] Wang, B., Cheng, G., n.d. Design of Cellular Structure for Optimum Efficiency of Heat Dissipation, in: Solid Mechanics and Its Applications. Springer Netherlands, pp. 107–116.https://doi.org/10.1007/1-4020-4752-5_11

[50] Wang, B., Zhou, S., Zhao, J., Chen, X., 2011. A size-dependent Kirchhoff microplate model based on strain gradient elasticity theory. European Journal of Mechanics - A/Solids 30, 517–524.https://doi.org/10.1016/j.euromechsol.2011.04.001

[51] Wang, D., Yang, Y., Liu, R., Xiao, D., Sun, J., 2013. Study on the designing rules and processability of porous structure based on selective laser melting (SLM). Journal of Materials Processing Technology 213, 1734–1742.https://doi.org/10.1016/j.jmatprotec.2013.05.001

[52] Wang, X., Zhang, P., Ludwick, S., Belski, E., To, A.C., 2018. Natural frequency optimization of 3D printed variable-density honeycomb structure via a homogenization-based approach. Additive Manufacturing 20, 189–198.https://doi.org/10.1016/j.addma.2017.10.001

[53] Weisstein, Eric W. "Lattice Graph." From MathWorld–A Wolfram Web Resource. http://mathworld.wolfram.com/LatticeGraph.html

[54] Weisstein, Eric W. "Tiling." From MathWorld–A Wolfram Web Resource. http://mathworld.wolfram.com/Tiling.html

[55] Winter, R.E., Cotton, M., Harris, E.J., Maw, J.R., Chapman, D.J., Eakins, D.E., McShane, G., 2014. Plate-impact loading of cellular structures formed by selective laser melting. Modelling and Simulation in Materials Science and Engineering 22, 25021.https://doi.org/10.1088/0965-0393/22/2/025021

[56] Wong, M., Owen, I., Sutcliffe, C.J., Puri, A., 2009. Convective heat transfer and pressure losses across novel heat sinks fabricated by Selective Laser Melting. International Journal of Heat and Mass Transfer 52, 281–288.https://doi.org/10.1016/j.ijheatmasstransfer.2008.06.002

[57] Yang, Y., Zhao, L., Qi, D., Shan, M., Zhang, J., 2019. A fuzzy optimization method for octet-truss lattices. Rapid Prototyping Journal.https://doi.org/10.1108/rpj-10-2017-0212

[58] Zegard, T., Paulino, G.H., 2014. GRAND — Ground structure based topology optimization for arbitrary 2D domains using MATLAB. Structural and Multidisciplinary Optimization 50, 861–882.https://doi.org/10.1007/s00158-014-1085-z

[59] Zegard, T., Paulino, G.H., 2015. GRAND3 — Ground structure based topology optimization for arbitrary 3D domains using MATLAB. Structural and Multidisciplinary Optimization 52, 1161–1184.https://doi.org/10.1007/s00158-015-1284-2

[60] Zhang, C.H., Hu, Z., Gao, G., Zhao, S., Huang, Y.D., 2013. Damping behavior and acoustic performance of polyurethane/lead zirconate titanate ceramic composites. Materials Design 46, 503–510.https://doi.org/10.1016/j.matdes.2012.10.015

[61] Zhang, P., Toman, J., Yu, Y., Biyikli, E., Kirca, M., Chmielus, M., To, A.C., 2014. Efficient Design-Optimization of Variable-Density Hexagonal Cellular Structure by Additive Manufacturing: Theory and Validation. Journal of Manufacturing Science and Engineering 137, 21004.https://doi.org/10.1115/1.4028724

[62] YouTube. (2019). Lattice cube. [online] Available at:https://www.youtube.com/watch?v=qxGwKU_8EDk [Accessed 29 Jul. 2019].

[63] Carbon. (2019). Carbon lattice innovation — the adidas story - Carbon. [online] Available at:https://tinyurl.com/y8n472bs [Accessed 29 Jul. 2019].

[64] Khakalo, S., Balobanov, V., Niiranen, J., 2018. Modelling size-dependent bending, buckling and vibrations of 2D triangular lattices by strain gradient elasticity models: Applications to sandwich beams and auxetics. International Journal of Engineering Science 127, 33–52.https://doi.org/10.1016/j.ijengsci.2018.02.004

[65] Balobanov, V., 2018. Computational structural mechanics within strain gradient elasticity: mathematical formulations and isogeometric analysis for metamaterial design.

[66] Chen, M., Jiang, H., Zhang, H., Li, D., Wang, Y., 2018. Design of an acoustic superlens using single-phase metamaterials with a star-shaped lattice structure. Scientific Reports 8.https://doi.org/10.1038/s41598-018-19374-2

[67] Medium. (2019). An Overview of Monte Carlo Methods. [online] Available at:https://towardsdatascience.com/an-overview-of-monte-carlo-methods-675384eb1694 [Accessed 29 Jul. 2019].

[68] Anon, (2019). [online] Available at: http://web.mst.edu/~dux/repository/me360/me360_presentation.html, Chapter 8. Mechanical Aerospace Engineering, Missouri University of Science and Technology [Accessed 29 Jul. 2019].

[69] Niiranen, J., 2007. A Priori and a Posteriori Error Analysis of Finite Element Methods for Plate Models. 978-951-22-9003-1.

[70] Mei, C. Vernescu, B., 2010. Homogenization methods for multiscale mechanics. 10.1142/7427.

[71] Maranganti, R., Sharma, P., 2007. Length Scales at which Classical Elasticity Breaks Down for Various Materials. Physical Review Letters 98.https://doi.org/10.1103/physrevlett.98.195504

[72] Niiranen, J., Balobanov, V., Kiendl, J., Hosseini, S., 2017. Variational formulations, model comparisons and numerical methods for Euler–Bernoulli micro- and nano-beam models. Mathematics and Mechanics of Solids 24, 312–335.https://doi.org/10.1177/1081286517739669

[73] Doyle, J.., 1969. A general solution for strain-gradient elasticity theory. Journal of Mathematical Analysis and Applications 27, 171–180. https://doi.org/10.1016/0022-247x(69)90072-9

[74] Ashby, M.F., 2011. Designing Hybrid Materials, in: Materials Selection in Mechanical Design. Elsevier, pp. 299–340. https://doi.org/10.1016/b978-1-85617-663-7.00011-4

[75] Refai, K., Montemurro, M., Brugger, C., Saintier, N., 2019. Determination of the effective elastic properties of titanium lattice structures. Mechanics of Advanced Materials and Structures 1–14. https://doi.org/10.1080/15376494.2018.1536816

A APPENDIX: Additional figures

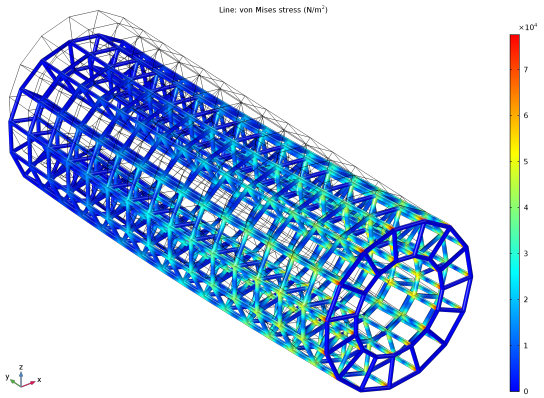

(a) Case 1, perspective view

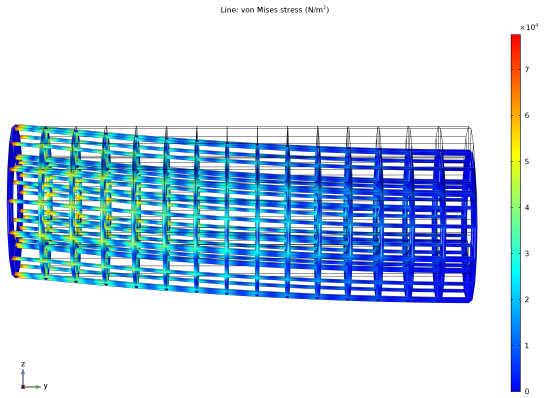

(b) Case 1, lateral view

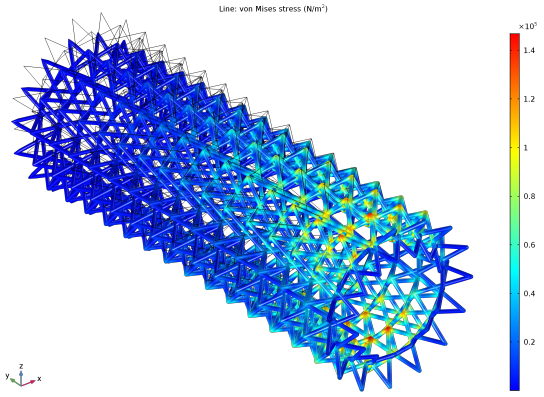

(c) Case 2, perspective view

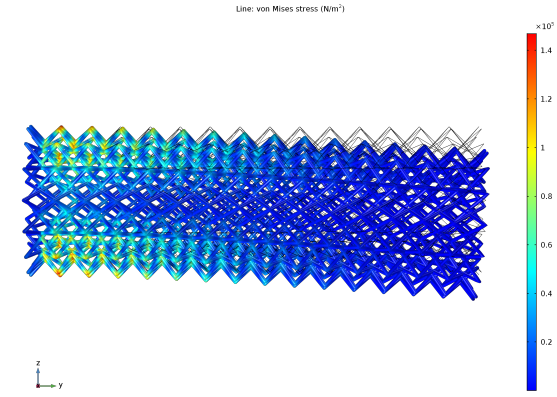

(d) Case 2, lateral view

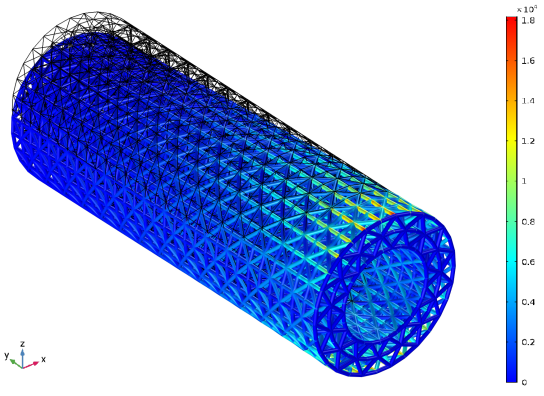

(e) Case 3, perspective view

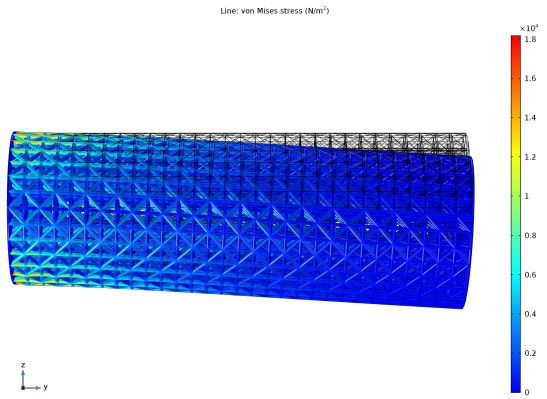

(f) Case 3, lateral view

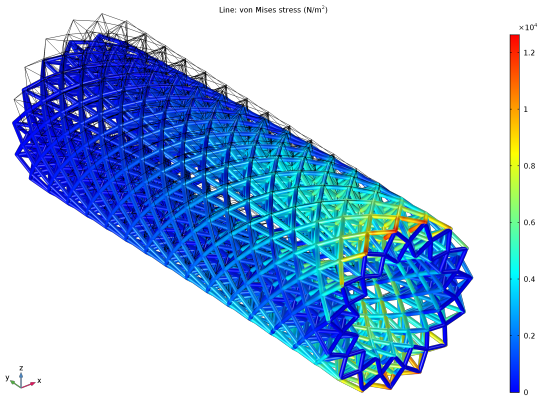

(g) Case 4, perspective view

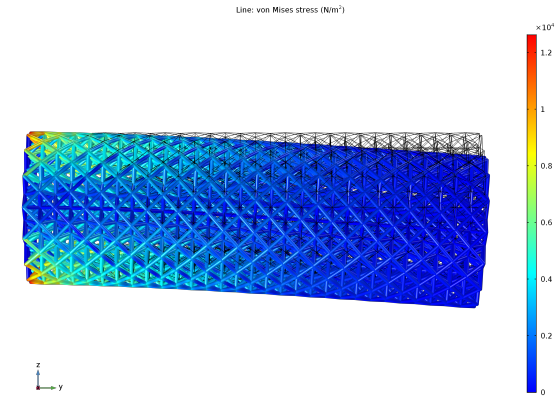

(h) Case 4, lateral view

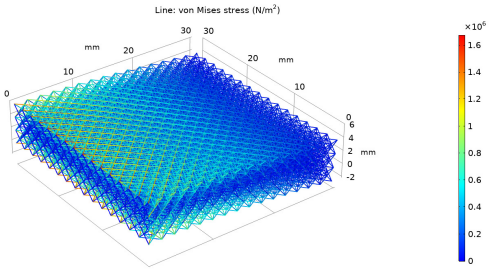

(a) Case 1, perspective view

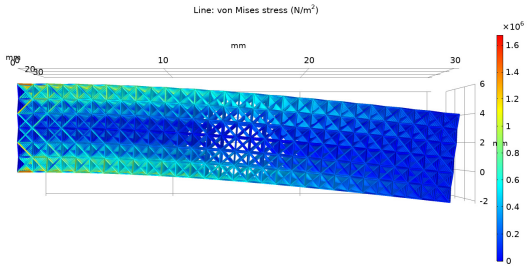

(b) Case 1, lateral view

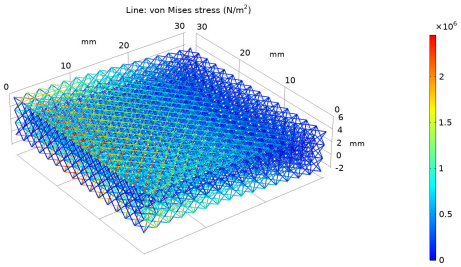

(c) Case 2, perspective view

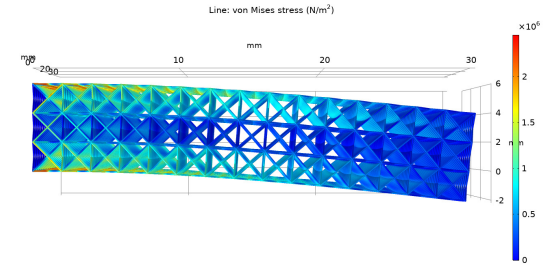

(d) Case 2, lateral view

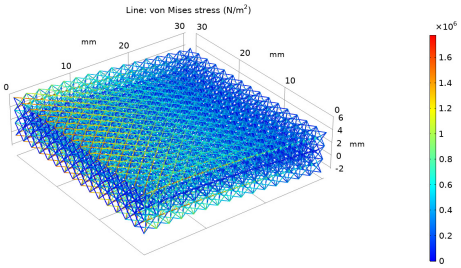

(e) Case 3, perspective view

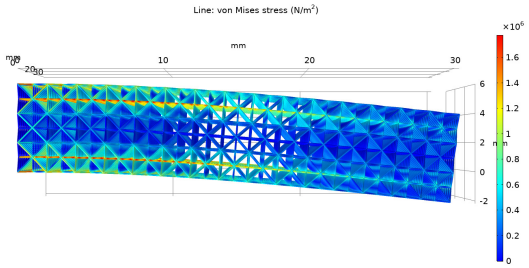

(f) Case 3, lateral view

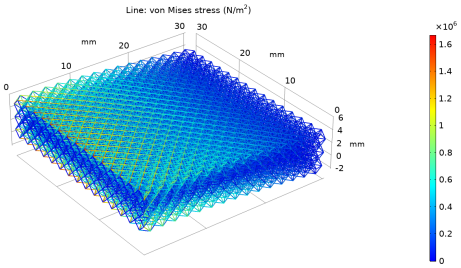

(g) Case 4, perspective view

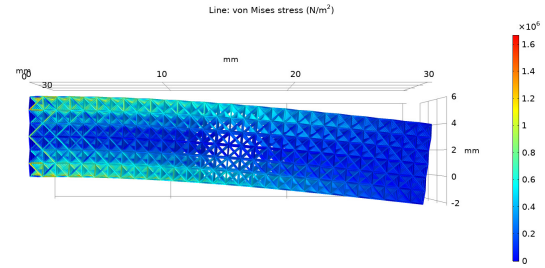

(h) Case 4, lateral view

Figure A2: Resulting Von Misses stress state of four different lattice plates. Subfigure a) and b) correspond to the cubic pattern, figure c) and d) correspond to the X-shape pattern, e) and f) correspond to the six-tetrahedral-cube pattern and figure g) and i) correspond to the octet-truss pattern.